Article:

World Scientific
www.worldscientific.com

Biological modeling with nonlocal advection–diffusion equations

Kevin J. Painter ⓘ*

Dipartimento Interateneo di Scienze,
Progetto e Politiche del Territorio (DIST),
Politecnico di Torino, Italy
kevin.painter@polito.it

Thomas Hillen ⓘ

Department of Mathematical and Statistical Sciences,
University of Alberta, Canada
thillen@ualberta.ca

Jonathan R. Potts ⓘ

School of Mathematics and Statistics,
University of Sheffield, UK
j.potts@sheffield.ac.uk

The employment of nonlocal PDE models to describe biological aggregation and other phenomena has gained considerable traction in recent years. For cell populations, these methods grant a means of accommodating essential elements such as cell adhesion, critical to the development and structure of tissues. For animals, they can be used to describe how the nearby presence of conspecifics and/or heterospecifics influence movement behaviour. In this review, we will focus on classes of biological movement models in which the advective (or directed) component to motion is governed by an integral term that accounts for how the surrounding distribution(s) of the population(s) impact on a member's movement. We recount the fundamental motivation for these models: the intrinsic capacity of cell populations to self-organise and spatially sort within tissues; the wide-ranging tendency of animals towards spatial structuring, from the formations of herds and swarms to territorial segregation. We examine the derivation of these models from an individual level, illustrating in the process methods that allow models to

*Corresponding author.

be connected to data. We explore a growing analytical literature, including methods of stability and bifurcation analysis, and existence results. We conclude with a short section that lays out some future challenges and connections to the modelling of sociological phenomena including opinion dynamics.

Keywords: Nonlocal PDEs; interacting particles; aggregation, flocking and swarming; sorting; territory formation.

AMS Subject Classification 2020: 92B05, 92C17, 92D40, 92C15

1. Introduction

A flamboyance of flamingos, a shiver of sharks, a confusion of wildebeest; hundreds of collective nouns have been assigned to define the groups formed by different species. The need for these collective nouns reflects the frequency with which animal groups form across the natural world, from the gathering of a small number of individuals to billions-strong swarms of locusts[182] or a herring shoal that stretches across kilometres.[132] An ability to aggregate is a phenomenon that extends down to the microscopic level, where various bacteria[30, 31] and microorganisms[26] have been observed to organise into aggregates under certain conditions. In the context of our own cells, their capacity to bind and organise is key for the development of many tissues and organs, or their repair following injury.

An essential element in the formation of many groups is the triggering of a movement-based response in an individual, according to signals and behaviours of other members. Directly, a cell may touch another cell and pass information through specialised molecules at the cell surface, or a bird may alter its flight path according to the trajectory of a neighbour. Indirectly, cells may alter motility according to a molecular signal deposited by another cell and animals may respond to territorial scent markings of conspecifics. The cumulative effect of these individual-level behaviours can result in self-organisation at the population scale, for example the rounding up of an initially dispersed population into an aggregate or the adoption of some swarm configuration.

Scientific interest in self-organising phenomena has a long history, and the field forms a pillar of mathematical biology.[150] Naturally, much of the modelling within this field is indebted to the remarkable work[204] of Alan Turing through his reaction–diffusion model, proposed to explain how morphogenesis could occur. Turing's model involved only molecular components, and showed how an interplay between reaction and diffusion could break the symmetry of a spatially uniform distribution by amplifying natural stochastic fluctuations into an ordered and patterned state. This not only offered a plausible chemical blueprint for how a tissue could become patterned, but also a mathematical blueprint for determining whether self-organisation can occur in a system. Inspired by the aggregation mounds formed from starving *Dictyostelium discoideum* cells — the initiating step during a multicellular transformation that serves as a paradigm of self-organisation at the microscopic scale[26] — the celebrated chemotaxis model of Keller and Segel[117] followed Turing's

template to illustrate how a system that includes an actively migrating population could also undergo self-organisation. It shows that the positive feedback loop of chemotaxis to a self-secreted attractant could lead to mound formation.

Continuous biological movement models are often formulated as an advection–diffusion equation,[150] i.e.

$$\partial_t u(\mathbf{x}, t) = \nabla \cdot [D \nabla u(\mathbf{x}, t) - \mathbf{a} u(\mathbf{x}, t)], \tag{1.1}$$

where $u(\mathbf{x}, t)$ represents the density of some population at position $\mathbf{x} \in \Omega \subset \mathbb{R}^n$ and time $t \in [0, \infty)$. D measures the diffusive (undirected) component to movement, while $\mathbf{a}$ is an n-dimensional vector that measures the advective (directed) component to movement. Generally, diffusion may be an $n \times n$ diffusion tensor matrix, e.g. describing some anisotropic spread due to the environment,[101] however here we will generally take an isotropic diffusion represented by a scalar coefficient d, so that $D = d I_n$ where I_n is the $n \times n$ identity matrix. The region Ω defines the space in which the population moves: this could range from a line if movement is effectively constrained to a one-dimensional geometry ($n = 1$, e.g. cell movement along nano-engineered channels), a two-dimensional surface ($n = 2$, e.g. animal movement across a landscape) to a three-dimensional volume ($n = 3$). If Ω is a bounded domain, then the above model (1.1) will be equipped with appropriate boundary conditions.

For the chemotaxis model of Keller and Segel[117] interactions between individuals are indirect: the individual senses (and moves in response to) another individual through following the local gradient of an attractant secreted by the population. As such, the advective velocity is taken to be proportional to the chemoattractant gradient, i.e. $\mathbf{a} \propto \nabla v$, where v is the attractant.

In other instances of group formation, however, interactions are direct: molecular binding between receptors on adjacent cell surfaces can lead to cells pulling themselves together (adhesion or attraction) or moving away from each other (repulsion); animals may also be drawn to each other or move away following a visual sighting of conspecifics. In all such instances, the interaction range becomes a crucial point for consideration: in the case of cells, this could be the range over which a cell can contact a neighbouring cell through touch, or, for animals, the range over which the perception of conspecifics influences its movement behaviour.

Given the existence of an interaction range, an individual has the potential to sense multiple neighbours simultaneously. It is natural, therefore, to suppose that the movement will be based on some integrated response, i.e. according to the distribution of a population (or populations) across its interaction range. Such considerations have led to the increasing adoption of nonlocal PDE formulations.[51] The focus of attention in the present review will be on models in which the nonlocality appears within the advective term, which is calculated according to an integral that measures the influence of the surrounding population on movement. Specifically,

we consider the following pair of nonlocal models,

$$\partial_t u = d\Delta u - \mu\nabla\cdot[u\mathbf{k}_R * f], \quad \mathbf{k}_R * f(\mathbf{x}, t) = \int_\Omega \mathbf{k}_R(\mathbf{x}, \mathbf{y})f(u(\mathbf{y}, t))d\mathbf{y}, \quad (1.2a)$$

$$\partial_t u = d\Delta u - \nu\nabla\cdot[u\nabla(w_R * g)], \quad w_R * g(\mathbf{x}, t) = \int_\Omega w_R(\mathbf{x}, \mathbf{y})g(u(\mathbf{y}, t))d\mathbf{y}. \quad (1.2b)$$

Motivation for these two model forms can be found through a purely phenomenological argument or by applying a more physical-based reasoning.

Consider first the formulation (1.2a) and its phenomenological motivation (see top row of Fig. 1). Here, the nonlocal advection term is founded on the principal that the population at position $\mathbf{y}$ influences the movements of those at $\mathbf{x}$. The induced direction of movement and its magnitude depends on the product of a (vector-valued) function $\mathbf{k}_R(\mathbf{x}, \mathbf{y})$ and a (scalar-valued) function $f(u(\mathbf{y}, t))$. Specifically, $\mathbf{k}_R(\mathbf{x}, \mathbf{y})$ specifies a dependence on the distance of $\mathbf{y}$ to $\mathbf{x}$ and it identifies the direction of interaction. The function $f(u(\mathbf{y}, t))$ defines the dependence on the
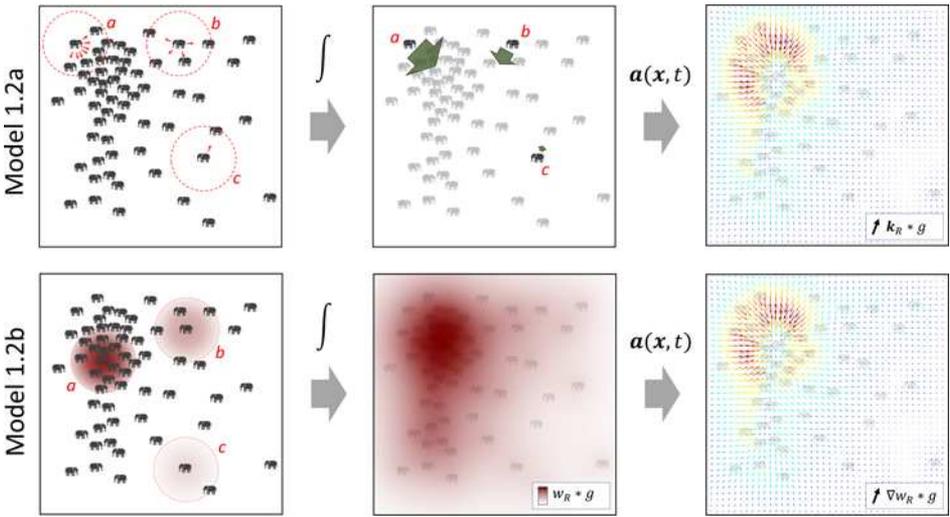
Fig. 1.   Illustration of the models (1.2) as formulated to describe grouping or herding, i.e. a tendency to move towards and aggregate at areas of higher population density. (Top row) For (1.2a) each individual within the interaction region (dotted circles) generates a local 'force' of attraction (top left); the number and direction will be different according to each individual's position (points a, b, c). Integrating over the interaction region leads to a net movement, the strength and direction varying with position (top middle). Overall, this generates an advective field that directs population-level movement (top right). (Bottom row) For (1.2b) an individual measures the (nonlocal) population density, e.g. by assessing the number of neighbours within the interaction region; at distinct positions (a, b, c), different numbers of neighbours will be detected (bottom left). Across space, this creates a population distribution map (bottom middle). The advective field for the population is according to the gradient of this distribution map (bottom right), e.g. in the direction of increasing gradient to describe a herding phenomenon. The advection fields generated through these two formulations have a similar form.

population size at $\mathbf{y}$. The integral kernel $\mathbf{k}_R$ is parametrised according to a sampling radius R, representing the interaction range. Net movement results from integrating over all possible positions, and this directly informs the advective velocity at $\mathbf{x}$. The parameters $d \in \mathbb{R}^+$ and $\mu \in \mathbb{R}$ describe diffusion and advection coefficients, respectively.

The phenomenological motivation for (1.2b) follows a similar reasoning (see bottom row of Fig. 1), although the function $w_R(\mathbf{x}, \mathbf{y})$ is now scalar-valued, as is the integrated quantity $w_R * g$. This formulation can be interpreted analogously to the taxis-like model, with the population moving according to the gradient of a nonlocal measure of the population; for example, this could be a nonlocally averaged density distribution. Again, the parameters $d \in \mathbb{R}^+$ and $\nu \in \mathbb{R}$ represent diffusion and advection coefficients, respectively.

A physical reasoning for (1.2a) and (1.2b) follows the consideration of forces and energies; this interpretation takes on particular resonance in the context of cell migration, where translocation of a cell's body stems from forces exerted as it attaches to other cells and the substrate. Model (1.2a) can be derived through a balance between adhesive and repulsive forces that act at the cell surface (e.g. see Ref. 38): interactions between cells centred at $\mathbf{x}$ and $\mathbf{y}$ generate local forces, with the net force according to the integral $\mathbf{k}_R * f$. This quantity hence describes a force density, with units of N/m, and the coefficient μ has units of $(sN)^{-1}$. The corresponding term for (1.2b) is $\nabla(w_R * g)$, and $w_R * g$ will carry the units of an energy density (J/m). Viewed in this light, the advection according to $\nabla(w_R * u)$ defines a movement according to an energy gradient. The summary review of Ref. 42 describes the derivations of models (1.2b) according to an energy principle. If the underlying principal is a process of energy minimisation (i.e. down the energy gradient) then parameter $\nu < 0$ and, conventionally, the form (1.2b) is written with the sign of the advection term reversed, i.e.

$$\partial_t u = d\Delta u + \gamma \nabla \cdot [u\nabla(w_R * g)], \quad w_R * g(\mathbf{x}, t) = \int_\Omega w_R(\mathbf{x}, \mathbf{y})g(u(\mathbf{y}, t))d\mathbf{y},$$

(1.3)

where $\gamma > 0$ indicates energy minimisation. Note that we will adopt this convention particular in Secs. 5.2 and 5.3, where energy-based analytical methods are utilised. Since energy differences lead to forces, a natural connection between these model forms is laid bare. A note of caution, though, must be applied when applying physical reasoning to biological particles such as animals or cells: attraction between conspecifics or avoidance of predators are measurable behaviours, but they cannot be directly related to a physical force or energy; similarly, a cell is a highly complex structure and its behaviour is not necessarily determined by the need to minimise energy.

Models of form (1.2) have been used since the 1970s to describe ecological systems (see Refs. 94, 116, 125, 140, 143, 152, 183 and 198), since the 1990s to describe cellular systems (see Refs. 8, 49, 81, 149 and 183), and more recently to describe

opinion dynamics (see Refs. 78 and 89). A particular point of mathematical interest lies in their capacity for self-organisation, in which modelling a process of self-to-self attraction between members can allow a dispersed population to organise itself into one or more aggregated groups. For this reason, they are commonly referred to as aggregation equations. However, it is important to note that the formulations (1.2) are less restrictive and can be used to model other forms of interaction, such as repulsive interactions that could lead to an enhanced dispersal.

Moreover, the form of these models can be extended to describe heterogeneous populations where the interactions between different populations can be distinct (e.g. see Refs. 8, 149, 158 and 175) or incorporated within more complicated models and applied to explain specific phenomena, such as cancer invasion for cellular systems (e.g. see Refs. 64, 81 and 157) or dynamics of locust swarms in ecological systems (see Refs. 79 and 199). A multi-species generalisation of each of the models (1.2a)–(1.2b) can easily be formed by extending to $\mathbf{u}(\mathbf{x}, t) = (u_1(\mathbf{x}, t), \ldots, u_p(\mathbf{x}, t))$, where u_i denotes the density distribution of the ith out of p populations, and considering the systems

$$\partial_t u_i = d_i \Delta u_i - \sum_{j=1}^{p} \mu_{ij} \nabla \cdot [u_i \mathbf{k}_{ij} * f_{ij}]$$

$$\mathbf{k}_{ij} * f_{ij} = \int_\Omega \mathbf{k}_{ij}(\mathbf{x}, \mathbf{y}) f_{ij}(\mathbf{u}(\mathbf{y}, t)) d\mathbf{y} \quad i = 1, \ldots, p, \qquad (1.4a)$$

$$\partial_t u_i = d_i \Delta u_i - \sum_{j=1}^{p} \nu_{ij} \nabla \cdot [u_i \nabla (w_{ij} * g_{ij})]$$

$$w_{ij} * g_{ij} = \int_\Omega w_{ij}(\mathbf{x}, \mathbf{y}) g_{ij}(\mathbf{u}(\mathbf{y}, t)) d\mathbf{y} \quad i = 1, \ldots, p. \qquad (1.4b)$$

In model (1.4a) directed movement is now the combined result of N movement-inducing interactions, where $\mathbf{k}_{ij} * f_{ij}$ is the nonlocal advection coefficient that defines the movement induced on members of population i due to interactions with population j: $\mathbf{k}_{ij}(\mathbf{x}, \mathbf{y})$ and $f_{ij}(\mathbf{u}(\mathbf{y}, t))$ are analogous to the functions described above, and parameters R_{ij}, d_i and μ_{ij} define the interaction range, diffusion coefficient and advection coefficients, respectively. Note that the μ_{ij}'s may be positive or negative, to model inter-species[175] or inter-cellular[158] attraction or repulsion, respectively. Analogous reasoning can be applied to the form (1.4b).

In this paper we review the increased employment of nonlocal systems of the above form within biological modelling.[a] In Secs. 2 and 3 we outline our motivating biological systems, namely cellular adhesion and other cell-based interactions (Sec. 2) and ecological interactions between animals (Sec. 3). We describe the

---

[a]Given the scope of this paper, we cannot cover all topics in detail and many relevant studies are omitted.

key biology and previous modelling that has motivated models of the form (1.2a) and (1.2b) or their multiple species extensions. In Sec. 4 we explore the derivations of these models from a microscopic perspective, in particular focussing on cellular adhesion. In Sec. 5 we consider some of the analyses used to understand these models, including linear stability analysis, bifurcation analysis and global existence. We conclude with some key challenges and future perspectives for the field.

2. Nonlocal Models for Cellular Systems

2.1. *Adhesion and other cell interactions*

Cell adhesion is the fundamental mechanism by which a cell attaches to and interacts with its surroundings.[3] Adhesions form through specialised cell surface receptors; their binding across adjacent membranes not only attaches cells together, but also triggers a range of processes from proliferation to migration. Of the various families of adhesion molecules, cadherins play a particularly prominent role within cell–cell adhesion processes (e.g. see Ref. 193): E-cadherins, for example, form tight adhesive junctions between epithelial cell types; N-cadherins are more commonly associated with transient adhesive interactions between motile mesenchymal cells.

Adhesion is critical for the organisation and maintenance of tissue structure. Naturally, cell–cell adhesion can lead to an accretion process, whereby contact between cells leads to attachment and the formation of a clustered population (Fig. 2(a)). Moreover, classic experiments indicate a role for adhesion in regulating the spatial organisation of different populations within a tissue.[200] In the differential adhesion hypothesis (DAH)[186, 202] cell sorting is suggested to result from distinct cell surface tensions, deriving in turn from the strength of adhesive interactions. The precise relationship leads to different configurations (see Fig. 2(b)), and experiments[77] for cell lines that express different levels of cadherins are consistent with this theory. More recently, measurements of the forces within adhesive aggregates[5, 202] have resulted in revision of the DAH to the differential interfacial tension hypothesis (DITH[29]): cell cortical contraction machinery and cell–cell adhesion combine to regulate interfacial tension, and sorting results from rearrangements that lead to a tissue-level minimisation of interfacial tension. Nevertheless, adhesion remains the driving force within the sorting and arrangement of tissues.

Cell-to-cell contacts, though, can also trigger repulsion. For example, contact inhibition of locomotion (CIL)[1] forms a contact-mediated response which not only leads to cessation of cell motion, but also repolarisation and reversal of the direction of motion.[41] Cell-to-cell contacts can also lead to asymmetric responses, where the two cells display contrasting responses. One such example arises in the pigmentation of zebrafish, where interacting xanthophores and melanophores engage in a chase and run[108, 219] interaction, contact between them resulting in
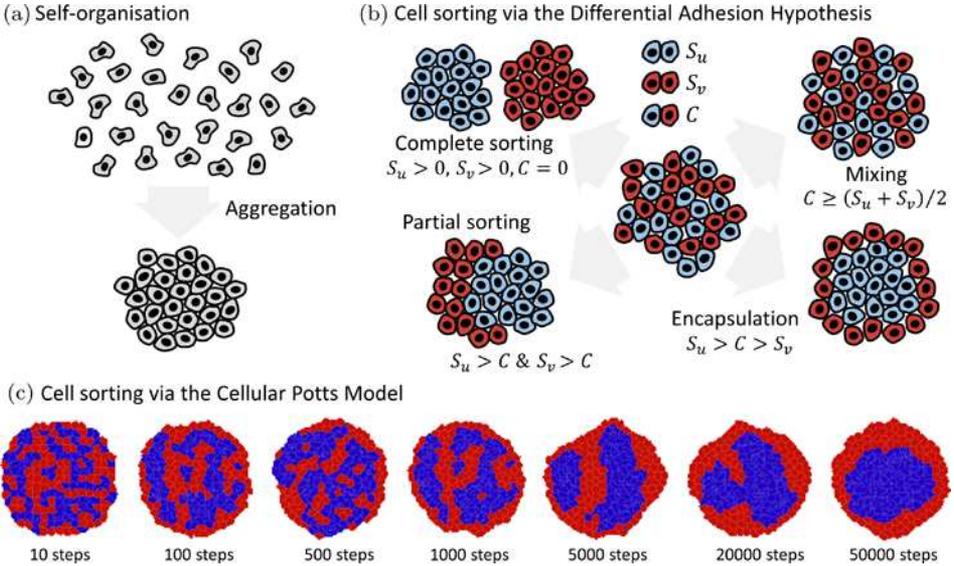
Fig. 2. (Color online) (a) Cell–cell adhesion naturally leads to accretion, with cells attaching on contact and forming a cluster or aggregation. (b) Sorting dynamics in adhesive populations, as predicted by the DAH. In a mixture of two distinct cell populations, three principal parameters can be identified: two self-adhesion strengths (S_u, S_v) and one cross-adhesion strength (C). The DAH predicts that different arrangements will arise according to the relationship between these parameters: for example, in a mixture of cells in which $S_u > C > S_v$, the u population (red) becomes encapsulated by the v (blue) population. (c) CPM simulation (implemented via Compu-Cell3D) showing encapsulation for a parameter setting in which adhesive interactions satisfy the aforementioned relationship.

the melanophore moving away from the pursuing xanthophore. Other instances of contact-mediated responses that can range from attraction to repulsion include those triggered through Eph/Ephrin interactions[36] or the chase and run dynamics observed in cultures of neural crest and placode cells.[196] A complex set of migration responses that follow direct contacts have been observed among cells of the immune system, impacting on a range of processes that include inflammation and tumor progression.[142]

Biological cells are typically small with average diameters the order of around ten microns and contact-based interactions occur at a similarly local level. However, contacts can also be formed at considerably greater distances than the mean cell diameter. First, the cell bodies can be highly deformable, where frequent protrusions of the membrane — pseudopodia[52] — locally extend parts of the membrane far beyond the average diameter. Second, a diversity of more specialised membrane protrusions have been identified[122, 181, 220] — variously termed cytonemes, tunnelling nanotubes, microtubes — that in some cases extend the order of 100s of microns. Thus, a contact can be achieved between cells separated by multiple cell diameters, and a nonlocal description is warranted.

2.2. *Models for adhesion and tissue dynamics*

2.2.1. *Individual-level models for adhesion and sorting*

Agent-based modelling (ABM) forms a natural approach for adhesive cell populations.[185, 189] The first broadly successful *in silico* replications of cell sorting can be attributed to Graner and Glazier,[87, 92] where a Potts model[b] was extended to model adhesion. Subsequently dubbed the Cellular Potts Model (CPM), each biological cell occupies multiple grid cells spread across a lattice, therefore giving each cell a shape, volume, and boundary. Evolution of the shape is probabilistically determined via a hypothesised energy functional; the aim is to minimise an energy determined by adhesive contacts along shared surfaces. Selecting relationships in line with the DAH leads to the predicted cell sorting pattern[87, 92]; see Fig. 2(c) for a CPM simulation in which adhesion relationships conspire to sort two populations into an encapsulated configuration.

Other ABMs have also shown to be capable of describing adhesion and sorting dynamics,[206] sitting at various levels of detail: cells modelled as deformable ellipsoids[161, 162] with centres and semi-axes evolving according to the forces generated by adhesive interactions with other cells and the substrate; on-lattice methods (e.g. cellular automata type, see Ref. 61); off-lattice centre-based models, where equations of motion describe the position and velocity of a cell's centre and the cell forms a hard or soft sphere that interacts with nearby cells (e.g. Refs. 45, 104 and 131); vertex-based models[74] which feature cell boundaries described by a polyhedron with dynamic vertices. Many of these ABMs form the basis of computational platforms for simulating cellular and tissue dynamics — CellSys,[c,104] CompuCell3D,[d,192] Chaste,[e,141] Physicell[f,83] — and their capacity to predict adhesion and sorting phenomena is regarded as a point of calibration between these diverse methodologies.[153]

2.3. *Continuous models for adhesion and sorting*

2.3.1. *Local formulations*

The representation of a cell population via a continuous density distribution eliminates the issue of scale inherent to agent-based models, where simulating very large cell numbers remains a computational challenge. Moreover, a well posed differential equation system gives access to a wealth of analytical methods (stability and bifurcation analysis, asymptotic approaches, travelling wave analyses) that can yield deeper understanding into the dynamics.

---

[b]A model of statistical mechanics, originally used to understand spin configurations in ferromagnets.
[c]https://www.hoehme.com/software/tisim.
[d]https://compucell3d.org/.
[e]https://www.cs.ox.ac.uk/chaste/.
[f]http://physicell.org/.

One simple approach to include adhesion has been based on a classic advection–diffusion equation of the form (1.1), where the diffusion and/or advection coefficients depend on the local population density, i.e. the pointwise density. Such models have been proposed on phenomenological grounds (e.g. see Ref. 105), or following a derivation from an underlying random walk description of movement (e.g. see Refs. 6 and 111) — see Sec. 4.1. These models capture certain features of adhesive populations — for example, restricted motility in regions of high adhesiveness — and are both analytically straightforward and simple to incorporate into models. Nevertheless, they have not been shown to allow more complicated sorting behaviour. Moreover, as discussed in greater detail below, the derived diffusion coefficients can sometimes become negative and result in a loss of regularity (for example Refs. 6 and 111). The effects of cell–cell adhesion have also been incorporated in a phenomenological manner into various models for tumor growth (for example Refs. 39, 40, 57, 58 and 217), via the incorporation of a surface tension force at the tumor-tissue surface.

2.3.2. *Nonlocal formulations*

Successful ABM approaches for cell sorting are inherently nonlocal: a cell spread across multiple lattice sites in a CPM, or centre-based approaches where the attractive and repulsive interactions form over an interaction range. This nonlocality can be incorporated into a continuum description using a nonlocal (or integral) PDE formulation. In the context of cell adhesion, the first[g] models to adopt this approach were formulated to describe the aggregation of a single homogeneous population in Ref. 183 and for multiple cell populations in Ref. 8 to explore sorting via differential adhesion; closely related nonlocal models, though, have a biomodelling history that dates back at least as far as the 1970s (for example see Refs. 94, 116, 140 and 151).

The simplest motivation for these models is founded on phenomenological reasoning. Suppose $u(\mathbf{x}, t)$ denotes the cellular density at position $\mathbf{x}$ in space and t in time. Ignoring (for simplicity) cellular growth or death and employing standard mass conservation arguments (e.g. see Ref. 150) lead to the balance equation

$$\partial_t u(\mathbf{x}, t) = -\nabla \cdot \mathbf{J}(\mathbf{x}, t),$$

where $\mathbf{J}(\mathbf{x}, t)$ denotes the population flux arising from movement. The flux can be decomposed into different terms — for example, a diffusive element to describe undirected movement and an advective component for directed movement — and we arrive at (1.1). Regarding the advective component, suppose that a cell at $\mathbf{x}$ interacts with another cell at $\mathbf{y}$, and that this interaction generates movement; this could be the result of forming adhesive bonds that draw the two cells together. The net movement response follows from summing over all possible interactions and we

---

[g]As far as we are aware.

then postulate an interactive flux proportional to this sum, i.e.

$$\mathbf{J}_{\text{interaction}} \propto u(\mathbf{x}, t) \int \mathbf{k}_R(\mathbf{x}, \mathbf{y}) f(u(\mathbf{y}, t)) d\mathbf{y},$$

where $\mathbf{k}_R$ and $f(u(\mathbf{y}, t))$ are as described following (1.2). Adding to the above a standard (Fickian) diffusive flux, $\mathbf{J}_{\text{diffusion}} = -d\nabla u$, leads to (1.2a).

A basic model to describe a homogeneous adhesive population sets $\mathbf{r} = \mathbf{y} - \mathbf{x}$,

$$\mathbf{k}_R(\mathbf{x}, \mathbf{x} + \mathbf{r}) = \chi_{|\mathbf{r}| < R} \vec{\mathbf{e}}_r \quad \text{and} \quad f(u(\mathbf{x} + \mathbf{r}, t)) \propto u(\mathbf{x} + \mathbf{r}), \tag{2.1}$$

where $\vec{\mathbf{e}}_r$ denotes the unit vector in direction of $\mathbf{r}$, and $\chi(\mathbf{r})$ is the indicator function. This stipulates (i) that only those cells within an interaction range R impact on movement, i.e. those within contact range for adhesive binding; and (ii) that the strength of interaction increases linearly with the density of cells at $\mathbf{x} + \mathbf{r}$, since a higher cell density implies a greater likelihood of forming adhesive bonds. Consequently, we obtain

$$\partial_t u = d\Delta u - \mu(R)\nabla \cdot \left(u \int_{B_R^n} u(\mathbf{x} + \mathbf{r}, t)\vec{\mathbf{e}}_r d\mathbf{r} \right), \tag{2.2}$$

where B_R^n is the n-dimensional ball of radius R. The coefficient $\mu > 0$ is a measure of the adhesive strength; switching to $\mu < 0$ turns the interaction into a repelling one, e.g. see Ref. 158 in the context of CIL. We note that often the function $\mathbf{k}_R$ is normalised, e.g. according to the volume of the interaction space and we therefore place a dependency on R in the parameter μ for generality. Other natural choices would be to assume that the strength of interaction decreases with increasing separation, due to reduced likelihood of forming a contact: for example, the magnitude of $\mathbf{k}$ decreasing exponentially with the distance $|\mathbf{r}|$. Nonlinear choices for f are also logical, e.g. forms to reflect an upper bound in the adhesive pull that can be generated, see below.

2.3.3. *Capacity for self-organisation and sorting*

A key strength in the model (2.2) lies in its capacity for self-organisation (see Sec. 5.1 for more details): for $\mu < \mu_{\text{crit}}$, a dispersed population remains dispersed (see Fig. 3(a)), while for $\mu > \mu_{\text{crit}}$ it becomes concentrated into a tight aggregate (see Fig. 3(b)). Under the basic model (2.2), the aggregates evolve into a highly concentrated aggregate,[h] even for $\mu \gtrsim \mu_{\text{crit}}$. This can be attributed to the lack of any mechanism that reins in the amount of adhesive pull that can be generated.

Adding further detail to the model assumptions can help prevent over-accumulation within the aggregates. For example, setting $f(u)$ to be a saturating function (which can be motivated naturally through adhesive receptor occupancy,

---

[h]For a discussion of global existence, see Sec. 5.2.

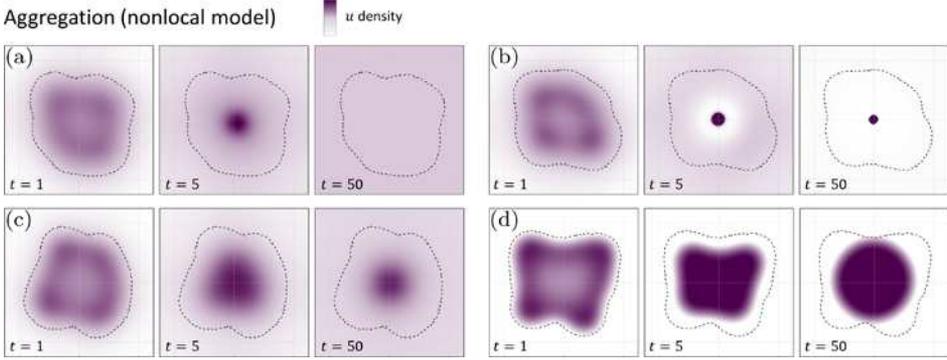Aggregation (nonlocal model)   *u* density

Fig. 3.   Self-organisation in a nonlocal model for adhesion, homogeneous population. The initial distribution sets a 'loose aggregate', the spatial extent of which is indicated by the dashed line in each frame. (a) Dispersal scenario for (2.2), with $d = R = 1$ and $\mu = 3.5/\pi$. (b) Aggregation for (2.2), with $d = R = 1$ and $\mu = 4/\pi$. (c) Aggregation for (2.3), for $d = R = K = 1$ and $\mu = 13.5/\pi$. (d) Aggregation for (2.4), for $d = R = K = 1$ and $\mu = 13.5/\pi$. The overall domain Ω is of size 10×10. We refer to Refs. 80 and 82 for details of the numerical implementation.

see Sec. 4), then

$$\partial_t u = d\Delta u - \mu(R)\nabla \cdot \left(u \int_{B_R^n} \frac{u(\mathbf{x} + \mathbf{r}, t)}{\kappa + u(\mathbf{x} + \mathbf{r}, t)} \vec{\mathbf{e}}_r d\mathbf{r} \right). \tag{2.3}$$

This leads to aggregations that are capped at lower densities (see Fig. 3(c)). Other possible modifications include the addition of 'volume-filling' (e.g. see Refs. 49 and 158), or adapting diffusion to a density-dependent and degenerate form (e.g. see Refs. 33, 34, 49, 145 and 149). The addition of the latter to (2.3) leads to

$$\partial_t u = d\nabla \cdot \left[u\nabla u - \mu(R) \left(u \int_{B_R^n} \frac{u(\mathbf{x} + \mathbf{r}, t)}{\kappa + u(\mathbf{x} + \mathbf{r}, t)} \vec{\mathbf{e}}_r \, d\mathbf{r} \right) \right]. \tag{2.4}$$

This adaptation limits a diffusive spread at the cluster boundary, the aggregate taking on a compact form with a sharp interface (Fig. 3(d)).

As noted earlier, nonlocal formulations can be easily extended to include multiple populations, see (1.4). A natural question, therefore, is whether cell sorting can be replicated under a nonlocal formulation. Consider two populations u and v and assume equivalently simple forms to (2.1), then a basic model to describe cell sorting can be stated by the equations

$$\partial_t u = d_u \Delta u - \nabla \cdot \left(u \int_{B_R^n} (S_u u(\mathbf{x} + \mathbf{r}, t) + Cv(\mathbf{x} + \mathbf{r}, t))\vec{\mathbf{e}}_r \, d\mathbf{r} \right), \tag{2.5a}$$

$$\partial_t v = d_v \Delta v - \nabla \cdot \left(v \int_{B_R^n} (S_v v(\mathbf{x} + \mathbf{r}, t) + Cu(\mathbf{x} + \mathbf{r}, t))\vec{\mathbf{e}}_r \, d\mathbf{r} \right). \tag{2.5b}$$

In this model S_u, S_v and C represent the u–u self-adhesion strength, the v–v self-adhesion strength, and the u–v cross-adhesion strength, respectively. Note that
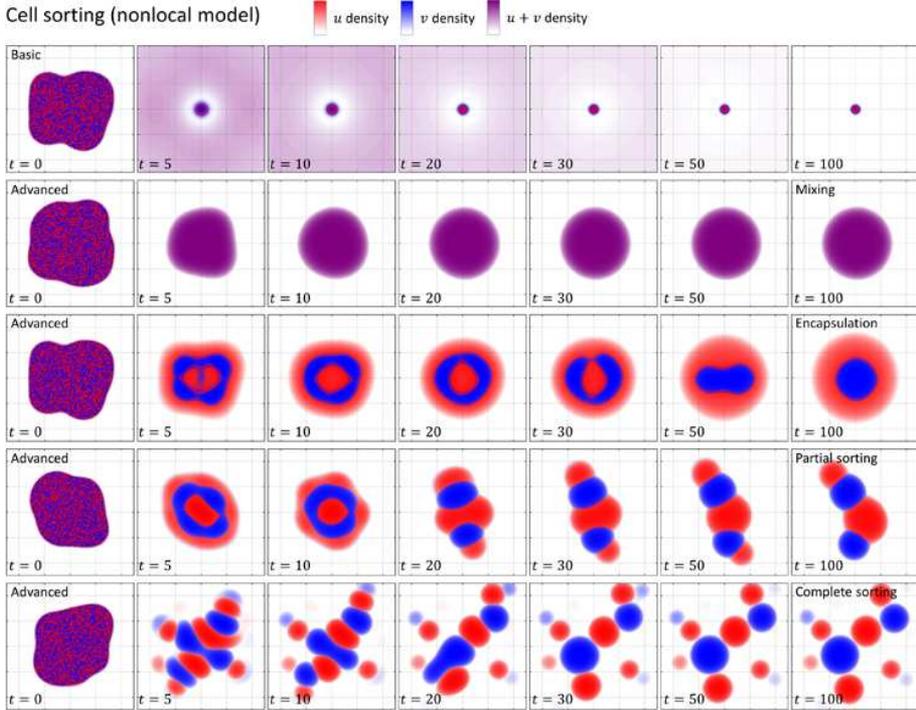
Fig. 4. Cell sorting in a nonlocal heterogeneous two population model for adhesion. Initially, the two populations are mixed within a loose aggregate, left column. First row shows a simulation of the basic model (2.5) under $S_u = 4$, $S_v = 1$, $C = 2$. Second to fifth rows show simulations of the advanced model (2.6) under the following scenarios: 'mixing' ($S_u = S_v = C = 8$, second row); 'encapsulation' ($S_u = 10$, $S_v = 4$, $C = 6$, third row); 'partial sorting' ($S_u = 10$, $S_v = 8$, $C = 3$, fourth row); 'complete sorting' ($S_u = S_v = 10$, $C = 0$, fifth row). All other parameters set at $d_u = d_v = R = \kappa_u = \kappa_v = 1$. The domain Ω is of size 10×10.

the interaction ranges are the same (and equal to R) and cross interactions are symmetrical, although such assumptions can be relaxed and repelling interactions can also be introduced (for example see Refs. 48 and 158). Unfortunately, this basic formulation (2.5) proves overly simple to capture the nuances of cell sorting. As for the basic homogeneous model (2.2), the linear choices for the nonlocal terms lead to excessive attraction and the populations become highly concentrated (see Fig. 4, top row). The model, as such, is unsatisfactory when it comes to resolving the subtly distinct cell sorting patterns shown in Fig. 2(b).

Consequently, 'successful' nonlocal models[8, 49, 82, 149, 158] that are more broadly capable of replicating the spectrum of arrangements predicted by the DAH include modifications to the various terms in model (2.5). For example, this has included adding biologically-meaningful features such as a limitation or saturation to the adhesive pull (see Refs. 8 and 82), introducing volume-filling effects that prevent cell aggregation beyond a critical (packed) level (see Refs. 49 and 158), or modifying diffusion terms to include total population pressure effects (see Refs. 34, 49 and 149).

To provide one concrete example, by adapting the saturating functional forms above
and including population-pressure effects to create sharply segregated boundaries
(see Refs. 49 and 149), we have

$$\partial_t u = \nabla \cdot \left[d_u u \nabla(u+v) - u \int_{B_R^n} \frac{S_u u(\mathbf{x}+\mathbf{r},t) + Cv(\mathbf{x}+\mathbf{r},t)}{\kappa_u + u(\mathbf{x}+\mathbf{r},t) + v(\mathbf{x}+\mathbf{r},t)} \vec{\mathbf{e}}_r \, d\mathbf{r} \right], \quad (2.6a)$$

$$\partial_t v = \nabla \cdot \left[d_v v \nabla(u+v) - v \int_{B_R^n} \frac{S_v v(\mathbf{x}+\mathbf{r},t) + Cu(\mathbf{x}+\mathbf{r},t)}{\kappa_v + u(\mathbf{x}+\mathbf{r},t) + v(\mathbf{x}+\mathbf{r},t)} \vec{\mathbf{e}}_r \, d\mathbf{r} \right]. \quad (2.6b)$$

This more 'advanced' sorting model is capable of replicating the nuances of cel-
lular sorting under different adhesive relationships, e.g. for two populations it can
generate the full spectrum of arrangements from mixed to complete sorting (see
Fig. 4).

Summarising, nonlocal models are capable of reaching two touchstones of adhe-
sive behaviour: (i) capturing the adhesive or sticky-like properties of cells in close
contact, and (ii) replicating cell-sorting phenomena for heterogeneous adhesive pop-
ulations as predicted by the DAH.

At this point we return to our earlier implication that local formulations are
incapable of adequately describing adhesion and sorting dynamics, stressing that
this applies to 'näive' local formulations. In fact, various local models can be shown
to exhibit sorting. One method (though not directly describing adhesion) is through
extension of a chemotaxis framework: effectively, a 'differential chemotaxis' system
in which two populations have distinct chemotactic responses to multiple chemical
factors (e.g. Refs. 121 and 156), so the interactions are indirectly mediated. Directly
relevant to adhesion, an intriguing (fourth order) local model has been recently
formulated in Ref. 71 and demonstrates an impressive capacity to simulate the
range of cell sorting patterns described here: we return to this in the discussion.

2.4. *Further applications to cellular systems*

Classic cell sorting experiments[200] were first performed using embryonic cell pop-
ulations, naturally leading to a conjecture that adhesion and sorting are funda-
mental during embryonic development (for a historial retrospective, see Ref. 187).
Consequently, a principal application for nonlocal models for cell adhesion lies
in developmental processes. In fact, the first nonlocal model for adhesion[183]
was proposed in the context of self-organisation of scale cells during lepidoptera
(moth and butterfly) wing morphogenesis. Nonlocal adhesion models have subse-
quently been developed, as described above, to show fundamental cell sorting (see
Refs. 8, 49, 82 and 149), somitogenesis,[i,9] skeletal morphogenesis,[j,23, 88] aspects of

---

[i]A fundamental early embryonic stage of segmented animals, whereby mesoderm tissue is sequen-
tially discretised into blocks of cells along the head to tail axis.
[j]The embryonic process during which the skeleton is formed.

neural development[133, 201] and vasculogenesis.[k,210] Notably, some of these applications have been directly formulated alongside experimental data, linking predictions formed from models to targeted experiments. For example, a nonlocal model of adhesion was formulated[23, 88] to describe mesenchymal cell movements which indicated a crucial aggregating role for adhesion during early skeletal morphogenesis. Experimental–theoretical studies that feature nonlocal adhesion models have also been used to understand brain development, in particular the crucial role of N-cadherin mediated adhesion in the positioning of neuronal populations during mammalian cortex development[133] and the visual centre of the fly *Drosophila melanogaster*.[201]

Abnormal regulation of adhesive processes may be a factor for various pathologies, in particular cancers.[109] For example, a point of significant focus has been on the epithelial–mesenchymal transition (EMT), where upregulation of N-cadherin accompanied by downregulation of E-cadherin allows cells to adopt a more migratory form, linked to increased invasiveness and metastasis.[128] Many mathematical models have been developed to address the roles played by cell–cell (and cell–matrix) adhesion during invasion and a growing number (e.g. Refs. 24, 25, 64, 81, 103, 119, 157 and 191) have applied nonlocal formulations: to understand how adhesion alters the shape of cancer invasion (e.g. Refs. 81 and 157); the role of cell–cell adhesion during glioma growth (e.g. Refs. 119 and 191); shaping different forms of tumor infiltration patterns in ductal carcinomas (see Ref. 64); and, two population models, featuring cancer populations at different states of mutation (see Refs. 24 and 25). Other points of application for nonlocal models of adhesion and cell interactions include wound healing (e.g. Refs. 65, 66, 213 and 214) and modelling the interactions between liver cells.[93]

3. Nonlocal Models for Ecological Systems

3.1. *Swarms, flocks and herds*

Swarming, herding and flocking phenomena are perhaps the most obvious examples of collective behaviour in ecological systems.[190] The central idea is that animals, like cells, often exhibit social interactions that cause them to aggregate. At their most basic level, social interactions may simply cause animals to be found in a particular area of space at some point in time, rather than using all the available area.[198] At a more advanced level, these interactions can cause a very wide range of complex patterns to emerge, famously exemplified by starling murmurations, but present throughout the animal kingdom.[12, 190]

An enormous number of models have been formulated to understand collective animal movements,[18, 209] a substantial proportion of which are based on systems

---

[k]Formation of the primitive vasculature network.

of 'interacting particles'[l]: the position of each agent is governed by a dynamic (usually, stochastic) equation featuring terms that account for how the trajectories of neighbours influence movement (well-known models include those in Refs. 7, 54, 55, 60, 96, 146, 179 and 208). Typically, the interactions lying at the heart of these models are formulated according to the 'first principles of swarming'.[46] At the shortest range, interactions are often repulsive, as animals will want to avoid physical contact. At a slightly longer range, animals will align their movements with one another. Then if animals become too far apart, they have a tendency to move towards one another to maintain the group cohesion (attraction). These three zones of nonlocal interactions[m] combine to give both stationary and moving aggregations, as well as a vast swathe of spatio-temporal patterns, mimicking many of those that have been observed in nature (see Refs. 18, 190 and 209).

A smaller — but still substantial — literature has approached the same central problem of swarming and animal movement via a continuous framework, using ideas that surround nonlocal advection (see Refs. 69, 143, 175, 198 and 211). In fact, the earliest nonlocal biological aggregation models were developed to describe swarming-like behaviour (see Refs. 116, 125, 140, 143 and 151) and were based on the nonlocal PDE (1.2a). For example, in Ref. 143 even or odd forms of interaction kernels were explored for their capacity to generate drift-type (coherent movement of the swarm) or aggregation-type (cohesion of the swarm) behaviour. A further branch of nonlocal PDE methods is founded on hyperbolic kinetic transport equations (see Refs. 20, 68 and 69). In these models, the nonlocal terms do not enter the advection terms, but the turning behaviour of the population; consequently, they benefit from a closer description of individual behaviour and can, for instance, explicitly incorporate the above principles of swarming commonly used in particle models. However, these models represent significant and nontrivial extensions of Eqs. (1.2)–(1.4) — although it is possible to connect them[32] — and are more challenging to explore from an analytical and numerical perspective. As such, we do not go into details, instead we refer the reader to a recent book[68] that summarises developments in this area.

---

[l]In probability theory, the term 'interacting particle system' has a specific definition in the context of continuous time Markov jump processes. When we refer to interacting particles within this paper, we will often slip into a slightly broader sense: complex systems composed of agents that interact with each other according to their relative positions and/or velocities.

[m]One of the earliest and most influential models explicitly built along these principles — the 'Boids' model of Reynolds[179] — was developed with the main aim of generating realistic flocking-like behaviour for the computer graphics industry, rather than the more elementary aim of understanding movement dynamics; numerous interactive online simulators of this model exist, e.g. https://boids.cubedhuang.com/. A particularly notable branch that evolved from that work was the application of swarming models to optimisation, i.e. particle swarm optimisation.[118]

3.2. *Home ranges and territories via stigmergy and memory*

As well as the visually impressive examples of collective movement, aggregation phenomena can also occur over longer spatial and temporal scales, becoming apparent as one observes animal locations over a period of time. For example, by plotting locations over an increasing time window, it often transpires that animals do not use as much of the available area as their locomotive capabilities allow. Instead they confine themselves to a smaller area called a home range, which they may maintain for a season or even a whole lifetime.[27, 35] This causes the spatial distribution of the animal to tend to a stationary, non-constant distribution, such as can be modelled by Eq. (1.2b) or variants thereof.[28]

Home ranges can emerge due to a range of biological processes. For example, animals may tend to re-visit locations remembered to be good for foraging.[180] Once they have memory of sufficiently many locations to meet their foraging needs, they may decide to stay in the vicinity of those locations (see Refs. 138 and 207). Additionally, they may need to construct a central place near to where they forage, such as a den or nest site, for reproductive purposes. The requirement to return to this central place then provides yet another mechanism of locational aggregation.[144] Finally, animals may leave traces of their past locations in the landscape (e.g. through scent marks) and use these as markers to keep them in their home range: a process called stigmergy.[195] In any of these cases, the decisions of the animal to move will tend to be spatially nonlocal, due to the animals' ability to sense their surroundings as they move, through sight, smell, or memory of target locations (see Refs. 14, 70 and 169).

To model these biological processes, it is common to couple a nonlocal advection–diffusion equation for the location distribution to an ordinary differential equation (ODE) modelling the process of memory or stigmergy. The recent review of Ref. 211 gives a thorough exposition of these processes, but perhaps the simplest example is

$$\partial_t u = d\Delta u - \nu\nabla \cdot (u\nabla w_R * m), \tag{3.1}$$

$$\partial_t m = \alpha u - \delta m, \tag{3.2}$$

where $u(\mathbf{x}, t)$ is the probability distribution of the animal and $m(\mathbf{x}, t)$ denotes the cognitive map,[211] which models either the density of marks left on the terrain or the amount of memory the animal has about location $\mathbf{x}$ at time t. Other notation is as in Eq. (1.2b).

Territoriality provides another reason why animals may confine themselves in space over long periods of time. Here, the presence of neighbouring conspecifics forces animals into a confined space (see Refs. 2 and 172). There are various mechanisms by which this can happen, but from a modelling perspective they fall into two categories. The first is via stigmergy: indirect interactions mediated by some form of marks on the terrain, such as urine, faeces, or a trail.[144, 174] In this case, animals avoid the marks left by others in the recent past, and usually these marks

decay over time. The second is via memory of direct interactions, such as displays or fights.[120] Animals remember the locations of these displays or fights and may tend to avoid them in the near future.[173] In either case, as with home range formation, the movement of animals in response to these interactions is usually spatially nonlocal.

These territorial mechanisms can be modelled using exactly the multi-population system in Eq. (1.4b) with $\nu_{ij} < 0$ for $i \neq j$ to model mutual avoidance, and $\nu_{ii} \geq 0$. However, as with home range models, it is often valuable to model the process of memory or stigmergy explicitly via ODEs. A simple example can be given by combining the ideas behind Eqs. (3.1) and (3.2) with those of Eq. (1.4b), as follows:

$$\partial_t u_i = d_i \Delta u_i - \nabla \cdot \left(u_i \nabla \sum_{j=1}^{p} \nu_{ij} w_R * m_j \right), \tag{3.3}$$

$$\partial_t m_i = \alpha u_i - \delta m_i, \tag{3.4}$$

where $m_i(\mathbf{x}, t)$ denotes the cognitive map of species i, and models the marks left by individuals from territorial unit i, whilst α and δ are constants. However more complicated versions can be considered that include extra biological realism.[173, 174, 211]

3.3. *A general framework for nonlocal interactions in ecology*

As well as territory formation, the multi-species case from Eq. (1.4) enables a variety of other ecological phenomena to be modelled over timescales where births and deaths are negligible (e.g. for mammals and birds, this may be over a season or year).[84, 175] For example, the movements of co-existing predators and prey can be modelled by assuming prey advect away from predators and predators towards prey.[62] Likewise, competing species may advect away from one another and mutualistic animals may have a tendency to move towards one another. In forager and scrounger interactions, the latter follow the former to exploit their foraging efforts (e.g. see Ref. 194). In ecosystems consisting of many species, there will be a complex network of such interactions that can cause a wide range of emergent patterns (Figs. 5(c)–5(e)).

As a consequence, Eq. (1.4b) has been proposed as a key study system for understanding spatial distributions of interacting groups of animals that may emerge over such timescales.[175] These groups of animals may be territorial groups, populations, or whole species. The overall aim is to be able to provide links between the network of interactions between moving species (Fig. 5(b)) and their pattern formation properties.

For example, Fig. 5(a) shows the predictions of linear stability analysis for four different systems of three populations (model (1.4b) for $i = 1, 2, 3$) shown schematically in Fig. 5(b). This gives a simple categorisation into 'no patterns'
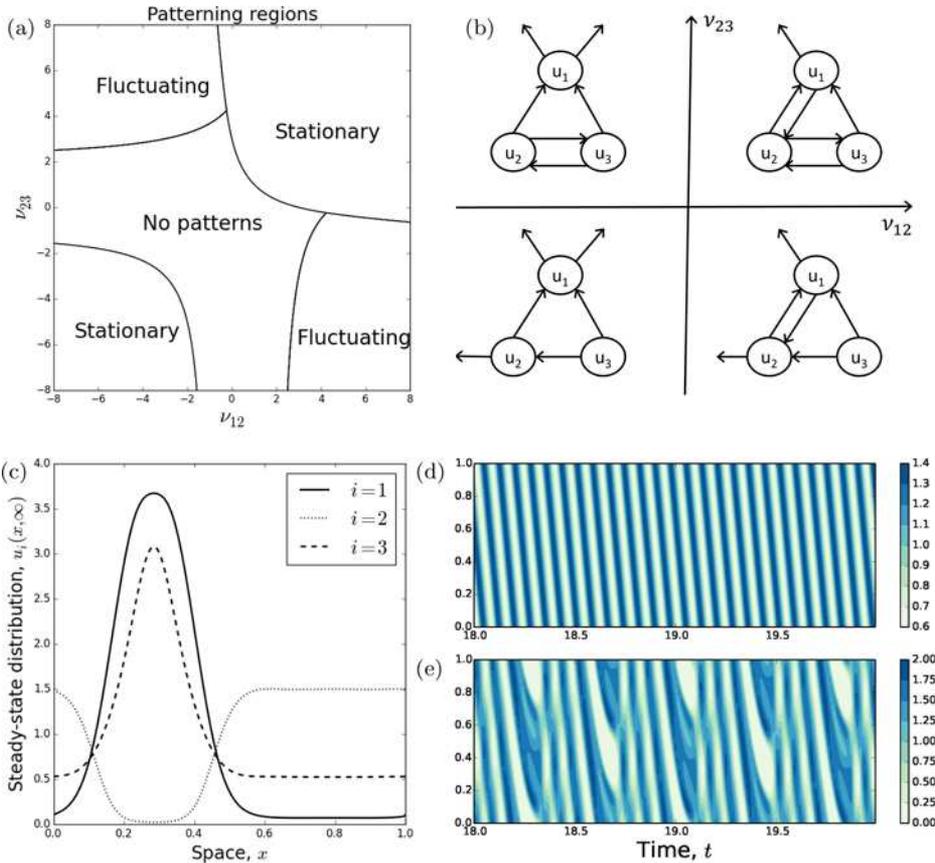
Fig. 5.   Patterns for example three-species model ecosystems of the form in Eq. (1.4b). Panel (a) gives the linear pattern formation regimes for systems described by Panel (b). In each system, an arrow from u_i to u_j means that u_i is attracted to u_j. An arrow away from u_i in the opposite direction from u_j means u_i avoids u_j. So, for example, the top-left graph in Panel (b) might model two mutualist predator species living alongside a single prey species. Panels (c)–(e) give numerical examples of the patterns that can form in a three-species system. In Panel (c), the system tends to a steady state where u_1 and u_3 aggregate together but are segregated from u_2. Panels (d) and (e) give example spatio-temporal patterns for u_1 with a three-species system. In all panels, $d_1 = d_2 = d_3 = \nu_{21} = \nu_{31} = \nu_{32} = 1$ and $\nu_{13} = -1$. In Panels (c)–(e), $\nu_{23} = -4$. Panels (c)–(e) have $\nu_{12} = -4$, $\nu_{12} = 3.3$ and $\nu_{12} = 4$, respectively.

(all eigenvalues having negative real parts) 'stationary patterns' (the dominant eigenvalue is real and positive) or 'fluctuating patterns' (the dominant eigenvalue is non-real with positive real part). However, further away from linear stability regime, patterns in three-population systems can be quite complex and varied, including stationary patterns of aggregation and segregation (Fig. 5(c)), travelling-wave-like solutions (Fig. 5(d)), perpetual irregular oscillations (Fig. 5(e)) and more.[85, 175]

4. Derivations from the Individual Level and Connecting to Data

4.1. *Random walks*

When Karl Pearson coined the term 'random walk' in 1905,[164] the central question involved biological movement: if, within a particular time step, each mosquito moves some distance in a randomly chosen angle, can we estimate the distribution of a mosquito infestation? Fundamental work by Patlak[163] extended the question to include biases from the environment and persistence. Across the last few decades a vast number of studies have aimed to connect the random walk movements performed by individuals to population-level measures and distributions, for both cell and animal movement (e.g. see Refs. 19, 53, 155 and 203). Specifying a position jump random walk (PJRW, see Refs. 53, 152, 155, 159 and 188) forms a particularly well-trodden path. In the context of the present review, this approach can be used to motivate both local and nonlocal models for aggregation.[38] To illustrate this, we first lay down a general formalism.

Let us consider the probability that a random walker has its centre at position $\mathbf{x}$ at time t. If we have a population of independent walkers, this probability can be equated with the population density $u(\mathbf{x}, t)$, and we maintain this notion. Note that the definition in terms of the centre implicitly assumes that the walker can have some finite extent, i.e. it is not necessarily a point object. For now we shall avoid any discussion of boundary conditions and assume an individual can move anywhere in space: movement is within $\Omega = \mathbb{R}^n$. The time continuous Master equation for the PJRW has the following form[107, 155, 205]:

$$\partial_t u(\mathbf{x}, t) = \lambda \int_\Omega [T(\mathbf{x}, \mathbf{y}) u(\mathbf{y}, t) - T(\mathbf{y}, \mathbf{x}) u(\mathbf{x}, t)] \, d\mathbf{y}, \tag{4.1}$$

where $T(\mathbf{x}, \mathbf{y})$ is a probability density function for a jump from $\mathbf{y} \in \mathbb{R}^n$ to $\mathbf{x} \in \mathbb{R}^n$. Note that T can depend on t, but we omit this dependency from the notation. $\lambda > 0$ is a rate parameter. We remark that individuals can remain at their current location through setting $T(\mathbf{x}, \mathbf{x}) > 0$, which we refer to as a zero-length jump. We follow the approach of Ref. 38 and rewrite the integral kernel $T(\mathbf{x}, \mathbf{y})$ according to the jump heading $\mathbf{z} = \mathbf{x} - \mathbf{y}$. Specifically,

$$T_\mathbf{y}(\mathbf{z}) := T(\mathbf{y} + \mathbf{z}, \mathbf{y}) = T(\mathbf{x}, \mathbf{y}), \quad \mathbf{z} = \mathbf{x} - \mathbf{y},$$

where we assume that

$$T_\mathbf{y} \geq 0, \quad T_\mathbf{y} \in L^1(\mathbb{R}^n), \quad \|T_\mathbf{y}\|_1 = 1.$$

$T_\mathbf{y}$ can be split into even and odd components,

$$E_\mathbf{y}(\mathbf{z}) = \frac{1}{2}(T_\mathbf{y}(\mathbf{z}) + T_\mathbf{y}(-\mathbf{z})), \quad O_\mathbf{y}(\mathbf{z}) = \frac{\mathbf{z}}{2|\mathbf{z}|}(T_\mathbf{y}(\mathbf{z}) - T_\mathbf{y}(-\mathbf{z})). \tag{4.2}$$

Then

$$T_\mathbf{y}(\mathbf{z}) = \begin{cases} E_\mathbf{y}(\mathbf{z}) + O_y(\mathbf{z}) \cdot \dfrac{\mathbf{z}}{|\mathbf{z}|} & \text{if } \mathbf{z} \neq 0, \\[2mm] E_\mathbf{y}(\mathbf{z}) & \text{if } \mathbf{z} = 0 \end{cases} \tag{4.3}$$

with an even part $E_{\mathbf{y}} \in L^1$ and an odd part $O_{\mathbf{y}} \in L^1$, which satisfy

$$E_{\mathbf{y}}(\mathbf{z}) = E_{\mathbf{y}}(-\mathbf{z}) \quad \text{and} \quad O_{\mathbf{y}}(\mathbf{z}) = O_{\mathbf{y}}(-\mathbf{z}). \tag{4.4}$$

We employ this decomposition in the general master equation (4.1) and make two further assumptions. First, that transition rates do not depend on the increment $\mathbf{z}$, just the starting location $\mathbf{y}$: this describes a myopic random walk. Second, non-zero-length jumps are small and of fixed length $h \ll 1$, and Taylor expansions can therefore be applied. Details of the expansions can be found in Ref. 38 where, in the limit as $h \to 0$ and $\lambda \to \infty$, we arrive at the advection–diffusion equation

$$\partial_t u(\mathbf{x}, t) + \nabla \cdot (\mathbf{a}(\mathbf{x}, t) u(x, t)) = \Delta(D(\mathbf{x}, t) u(\mathbf{x}, t)). \tag{4.5}$$

We denote by $\mathbb{S}^{n-1}$ the $n-1$-dimensional unit sphere in $\mathbb{R}^n$. The advection velocity is given by

$$\mathbf{a}(\mathbf{x}, t) = \lim_{h \to 0, \lambda \to \infty} \frac{\lambda h^n}{n} |\mathbb{S}^{n-1}| O_{\mathbf{x}},$$

and the diffusion term by

$$D(\mathbf{x}, t) = \lim_{h \to 0, \lambda \to \infty} \frac{\lambda h^{n+1}}{2n} |\mathbb{S}^{n-1}| E_{\mathbf{x}}.$$

Particular care must be paid to the limit scalings, as they suggest different powers of h: for the limits to simultaneously exist the odd part must be small (i.e. $O_{\mathbf{x}} \sim h$) with respect to the even part. If the odd part is of order one or larger, the diffusion term vanishes and a pure drift equation (a drift-dominated case) is derived. When the odd part is of order h^2 or smaller, the drift term vanishes and a diffusion-dominated case arises. The value of separating T with respect to its odd and even parts becomes clear: the even component $E_{\mathbf{x}}$ enters the diffusion term, while the odd component $O_{\mathbf{x}}$ determines the advection term. Generally the odd and even parts can involve nonlocal terms that represent sensing up to a certain radius. We will return to this in the next section but one.

4.1.1. *Local models*

We illustrate the above scaling through an interesting local case, which leads to taxis-type models. To introduce dependency according to some controlling factor, we take the standard assumption[188] of supposing that the jump probability distribution explicitly depends on a control species, which we denote by $c(\mathbf{x}, t)$. For simplicity, we will restrict in this section to a symmetrical case where we set $T_{\mathbf{y}}(\mathbf{z}) = f(c(\mathbf{y}, t))$ for all non-zero length jumps (i.e. T depends only locally on $\mathbf{y}$ through $f(c(\mathbf{y}, t))$). When movement occurs, all headings are chosen with equal probability, but this probability varies with the local level of the control species c. There is no odd component to T and the limiting equation (4.5) in this case is of the form

$$\partial_t u = d\Delta(f(c)u) = d\nabla \cdot [f(c)\nabla u + uf'(c)\nabla c]. \tag{4.6}$$

Therefore — despite an absence of directionality to the jump — a taxis-like process emerges at the macroscopic level: advection according to the gradient of c. The control species can be distinctly interpreted according to the movement process. For example, it may simply define a fixed environmental variability, e.g. regions where movement is easier or more difficult. It could also change according to the distribution of the population — for example, a scent deposited by an animal or a chemical released by a cell — and therefore defined by an evolution equation such as (3.2). We refer to Refs. 17 and 100 for detailed reviews on chemotaxis models.

Using cell adhesion as a case study, a simple but naïve approach would be to directly equate the control species with the population density. Specifically, we consider $c \equiv u$ and hence obtain the density-dependent diffusion equation

$$\partial_t u = \nabla[D(u)\nabla u] \quad \text{with } D(u) = d(f(u) + uf'(u)). \tag{4.7}$$

Considering the 'stickiness' property of adhesion, a logical choice for $f(u)$ would be a decreasing function that reflects reduced capacity to move as a cell forms adhesive attachments with its neighbours. For example, a choice $f(u) = \frac{1}{\kappa+u}$ results in $D(u) = \frac{d\kappa}{(\kappa+u)^2}$: this reduces diffusivity in regions of higher population density, and corresponds with certain choices[105] in macroscopic (phenomenological) approaches to adhesion.

Derivations of local models for adhesion that rely on the PJRW framework have been considered previously (e.g. see Refs. 6, 111 and 114). While more sophisticated than the above — for example, more complicated jump probabilities or accounting for correlations in movement — they essentially lead to the same result of a density-dependent diffusion equation. Clear advantages lie in that they can lead to models that can be fitted against experimental data (e.g. obtained from cell assays[112, 113]), and that the derived PDE form is relatively tractable, both analytically and numerically.

However, while density-dependent diffusion captures one expected consequence of adhesion, it is more questionable in the context of self-organisation or cell sorting phenomena. The possibility of biological aggregation within both the underlying discrete master equation and its corresponding continuous model has been considered in various studies (for example see Refs. 6, 106, 127 and 160), and for (4.7) it is straightforward to use linear stability analysis (see Sec. 5.1) to show that for (4.7) this will depend on the shape of $f(u)$: instability of the uniform steady state, and hence self-organising capacity, requires $f(u) + uf'(u) < 0$. This is not possible for $f(u) = \frac{1}{\kappa+u}$, but can be satisfied when $f(u) = \frac{1}{(\kappa+u)^q}$ for $q > 1$. However, at this point the PDE (4.7) will become illposed and unpractical for application.

4.1.2. *Nonlocal models*

Intuitively, it is the pointwise nature of the dynamics that proves problematic in the above. The random walker responded only to the strictly local information

acquired at its centre: it is a point particle, and the population can potentially become trapped at singular locations of 'infinite stickiness'.

A cell or organism, though, has a spatial extent and, even if interacting only through direct contact, will interact across some volume of space. This naturally leads to the question of how one can extend derivations from PJRWs in a manner that retains this nonlocality. We will again use cell adhesion as a case study and follow the approach in Ref. 38. As noted earlier, the formation of adhesion bonds between membranes leads to the generation of (local) forces that draw cells together; cellular membranes are highly dynamic, extending and retracting protrusions that span shorter (e.g. lamellipodia) and longer (e.g. filopodia) ranges. Adhesive attachments, therefore, can create forces at a position $\mathbf{x} + \mathbf{r}$ that act to displace a cell centred at $\mathbf{x}$ where the distance $\mathbf{r}$ is potentially several mean cell diameters away. The method in Ref. 38 is to consider a biased random walk where the bias results from summing over all possible local forces that can impact on the cell centred at $\mathbf{x}$, which enter the odd component of T in (4.3). Following the scaling, one obtains a nonlocal advection velocity of the form

$$\mathbf{a}(\mathbf{x}) = \underbrace{\mu}_{\text{Adhesive strength}} \int \underbrace{N_b(u(\mathbf{x}+\mathbf{r},t))}_{\text{Number of bonds}} \underbrace{S(u(\mathbf{x}+\mathbf{r},t))}_{\text{Free space}} \underbrace{\omega(|\mathbf{r}|)}_{\text{Cell extension}} \underbrace{\vec{\mathbf{e}}_r}_{\text{Direction}} d\mathbf{r}. \tag{4.8}$$

In the above, μ denotes an adhesive strength per adhesion bond, $\mathbf{r}$ denotes the direction and length of the cell extension, $N_b(u(\mathbf{x}+\mathbf{r},t))$ denotes the bound adhesion receptors that are generated with cells at location $\mathbf{x}+\mathbf{r}$, $S(u(\mathbf{x}+\mathbf{r},t))$ indicates the amount of free space available for cells to extend into this area, $\omega(|\mathbf{r}|)$ denotes the ability of a cell to express adhesion receptors a distance $|\mathbf{r}|$ away from its centre, and $\vec{\mathbf{e}}_r$ accounts for that bonds generated at $\mathbf{x}+\mathbf{r}$ will lead to a bias corresponding to that direction.

The formulation in (4.8) is rather general, therefore admitting varying degrees of biological detail. For example, assuming compact support for the cell extension, no space limitation ($S = 1$), and using mass action kinetics to set the number of bonds to be proportional to the cell density ($N_b(u) \propto u$), one essentially arrives at a model of the form (2.2). If, rather, one takes the adhesion binding to be governed by a Michaelis–Menten type binding mechanism, $N_b(u(\mathbf{x})) \propto \frac{u(\mathbf{x})}{\kappa + u(\mathbf{x})}$, then we arrive at a model similar to that specified in (2.3).

Consequently, through an explicit derivation from a PJRW it is possible to motivate and clarify the implicit assumptions that underlie various nonlocal models for adhesion, in particular those originally developed with phenomenological reasoning and applied to various phenomena (Sec. 2.4). More generally, given that the integral (4.8) will typically be a nonlinear function of the cell density $u(\mathbf{x} + \mathbf{r})$ and the ability to form attachments varies with the distance from the cell centre, one can straightforwardly obtain the general formulation in (1.2a).

4.1.3. *Step selection functions*: *Connecting to data on organism movement*

The formalism of a PJRW also allows for relatively straightforward parameterisation of advection–diffusion equations based on data, an approach that has been used both for experimental data obtained for cell systems (say, using cellular assays, e.g. Ref. 112) and locational data for animals (e.g. Refs. 170 and 177).

Taking the example of animal movement, these data typically arrive as a time series of locations. If this time series is relatively low frequency, e.g. of the order of one location every few minutes or hours, we might use the funtion $T(\mathbf{x}, \mathbf{y})$ (Eq. (4.1)) to model movement between successive measured locations, from $\mathbf{y}$ to $\mathbf{x}$ (see Ref. 75). Alternatively, if the time series is very high frequency, e.g. many locations per second, which is increasingly common,[215] $T(\mathbf{x}, \mathbf{y})$ can be used to model movements between successive places where the animal makes a turn.[148] In this latter case, we are more accurately modelling behavioural decisions of animals, as they will likely turn for a reason.[216]

Either way, a huge amount of ecological insight has been gained in recent years by fitting functions that describe a position-jump process to time series of animal location data (e.g. see Refs. 73, 76 and 197). Moreover, further understanding can be gained by scaling these processes up to distributions of broad-scale space use patterns via advection–diffusion equations, using similar techniques to those described in Sec. 4.1.[170] The specific position-jump model that has gained particular interest from the ecological community goes under the name 'step selection function' (SSF) and has the following form[n]

$$T(\mathbf{x}, \mathbf{y}) = \frac{\psi(\mathbf{x}, \mathbf{y})w(\mathbf{x}, \mathbf{y})}{\int_{\Omega} \psi(\mathbf{x}, \mathbf{y})w(\mathbf{x}, \mathbf{y})d\mathbf{x}}, \tag{4.9}$$

where $\psi(\mathbf{x}, \mathbf{y})$ represents something about the organism's movement capability, often a distribution of 'step lengths' $|\mathbf{x} - \mathbf{y}|$,[o] and $w(\mathbf{x}, \mathbf{y})$ is a 'weighting function' which encapsulates anything that covaries with movement. Typically, $w(\mathbf{x}, \mathbf{y})$ is written in the following exponential form

$$w(\mathbf{x}, \mathbf{y}) = \exp[\boldsymbol{\beta} \cdot \mathbf{Z}(\mathbf{x}, \mathbf{y})], \tag{4.10}$$

where $\mathbf{Z}(\mathbf{x}, \mathbf{y})$ is a vector of functions, each of which represents a movement covariate, and $\boldsymbol{\beta}$ is a vector denoting the relative contribution of the effect of each covariate on movement. In many practical examples of step selection, $\mathbf{Z}(\mathbf{x}, \mathbf{y})$ are simply static environmental features measured at the end point of the step (so $\mathbf{Z}(\mathbf{x}, \mathbf{y})$ can be written as $\mathbf{Z}(\mathbf{x})$) (see Refs. 73 and 197). However, they can also represent features along a step, such as barriers,[22] or dynamic quantities such as

---

[n]The nomenclature in the literature is not always consistent here. Sometimes SSF refers to Eq. (4.9), sometimes to the numerator of this equation, and sometimes just to the function $w(\mathbf{x}, \mathbf{y})$.
[o]More generally, ψ could be a distribution of step lengths and turning angles, so that ψ is dependent upon $\mathbf{x}$, $\mathbf{y}$, and also the bearing θ on which the animal travelled to $\mathbf{y}$. But to keep the exposition simple, we will assume here that ψ only depends upon $\mathbf{x}$ and $\mathbf{y}$.

memory[137] or the presence of other organisms.[171] Memory processes lead to self-interaction, which may give rise to a single species aggregation-type equation (1.2). If co-moving animals or interacting populations are being modelled, it is necessary to write a different step selection function for each entity (individual or population).[176] These coupled step selection functions then lead to multi-species equations, like Eq. (1.4).[177]

A reason for the popularity of the functional form in Eqs. (4.9) and (4.10) is that parametrisation can be done simply and quickly using conditional logistic regression. Details of this technique are given elsewhere (see Refs. 10 and 75), but in short it involves first approximating the integral in the denominator of Eq. (4.9) by sampling from ψ, and then recognising the resulting function as the likelihood of a case-control study where the samples are the controls.

Although there are many empirical studies using step selection functions to infer information about animal movement (e.g. see Refs. 73 and 197), there are far fewer that take the next step of deriving the associated advection–diffusion equation to understand broad-scale space use patterns.[170] Perhaps, the reason for this is that such studies combine empirically driven questions with relatively-advanced mathematical analysis, thus require strong interdiscplinary collaborations between applied mathematicians, empirical ecologists, and statisticians. The flip-side is that there is huge, fertile ground for mathematicians to collaborate with those ecologists involved in step selection studies, enhancing their data analysis and answering new scientific questions.[171]

4.2. *Derivations from interacting particle system models*

As mentioned earlier, many of the ABM-based approaches to cellular and animal aggregation phenomena fall into the broad class of systems of 'interacting particles'. Deriving continuous models from these models forms a very large field, and a growing literature has emerged in which nonlocal models related to (1.2) are obtained. It is significantly beyond the scope of this paper to provide a comprehensive examination of this literature. Rather, we provide a few apposite examples and refer to others (e.g. Refs. 46 and 147) for a more general review.

To provide some context, we consider the following concrete example[p] in one dimension; we refer to Refs. 78 and 147 for more details. Let the position $x_i(t)$ of agent i in a population of size N at time t be determined by the stochastic differential equation

$$dx_i = -\frac{1}{N}\sum_{j=1}^{N} a_{ij}(x_i - x_j)dt + \sigma dW_i(t). \tag{4.11}$$

---

[p]We note that this particular example comes from a model formulated for opinion dynamics, rather than biological aggregation. However, the underlying principles are the same: a tendency to converge, whether in position or opinion, when agents are sufficiently close.

In (4.11), the W_i's denote independent Brownian motions and model an uncertainty to the particle position (with strength σ). Interactions are incorporated through the summed term, where a_{ij} gives the strength of interaction between agents i and j; the $1/N$ factor averages across all possible interactions. This general form can be tailored to describe an attraction process between sufficiently close individuals — e.g. as relevant for cell adhesion — by setting the interaction to be a function of the distance of separation, $|x_i - x_j|$, with compact support: i.e. no attraction above a critical interaction range.

To obtain a continuous model, one can consider the following empirical probability measure for the positions of all agents at time t:

$$u^N(t) = \frac{1}{N} \sum_{i=1}^{N} \delta_{x_i(t)}(dx),$$

where $\delta_x(dx)$ is the Dirac measure with point mass at position x. Through application of mean field asymptotic theory, it can be shown[78] that as $N \to \infty$ the probability measure u^N (weakly) converges to a deterministic density u, which under certain conditions is governed by a nonlocal PDE of the form (1.2a).

A number of other derivations from IPS models have also led to equations related to (1.2). In one paper[139] the starting point was an off-lattice centre-based model (see Sec. 2.2.1), in which the motion of each particle is governed by Newton's second law of motion under viscous forces, forces from self-propulsion and forces from interactions. The latter allowed adhesion-type interactions to be included, which followed the standard assumption of varying with the degree of separation. A hierarchical system of N nonlocal PDEs was obtained to describe the distribution of a population of N interacting cells and, again following a mean field approximation, a nonlocal aggregation model of the form (1.2a) is obtained.

Nonlocal aggregation models of the form (1.2b) can also be motivated from an IPS (e.g. see Refs. 33 and 145). The motivation in Ref. 145 lay in the aggregating tendency of ants (*Polyergus rufescens*), with each ant's position evolving according to a stochastic differential equation driven by Brownian motion and an interaction drift; drift dominated over random wandering when other individuals enter an ant's interaction range. Both aggregating and repelling effects were included, with the former operating when another individual enters an attracting range and a repulsion term for when they become too close. Assuming a large population N, then in the limit $N \to \infty$ the following equation was derived for the population density:

$$\partial_t u = d\Delta u + \nabla \cdot [u\nabla u - u\nabla(w * u)],$$

where d follows from the Brownian motion and the density-dependent (degenerate diffusion) and nonlocal drift terms follow from the repulsion–attraction interaction; w derives from the aggregation interaction kernel. The above essentially combines the formulation (1.2b) with an additional degenerate diffusion term, as previously described in Sec. 2.3.3.

5. Analytical Properties

5.1. *Linear stability analyses*

A linear stability analysis can be used to demonstrate basic criteria for aggregation from a dispersed initial state, i.e. self-organisation properties. We first consider the formulation (1.2a) and, for maximum clarity, utilise the simple assumptions that lead to (2.2) and constrain to a one-dimensional infinite domain; the latter restriction circumvents the complications that arise from specific boundary conditions. Consequently, (2.2) becomes

$$\partial_t u = d\partial_{xx} u - \mu(R)\partial_x \left[u \left(\int_0^R u(x+y,t)dy - \int_0^R u(x-y,t)dy \right) \right], \quad (5.1)$$

while under equivalent assumptions the formulation (1.2b) becomes

$$\partial_t u = d\partial_{xx} u - \nu(R)\partial_x \left[u\partial_x \left(\int_{-R}^R u(x+y,t)dy \right) \right]. \quad (5.2)$$

Assuming that the population is initially distributed about a uniform steady state $\bar{u}$, we perform a Turing-type stability analysis (e.g. Ref. 150) by linearising about the uniform steady state and looking for solutions to the linearised equation with mode k and eigenvalue σ as $e^{ikx+\sigma t}$. This yields the characteristic equations for the eigenvalue–wavenumber relationship

$$\sigma = -dk^2 + 2\bar{u}\mu(R)(1-\cos(kR)) \quad \text{and} \quad \sigma = -dk^2 + 2\bar{u}\nu(R)k\sin(kR) \quad (5.3)$$

for (5.1) and (5.2), respectively. Inhomogeneous perturbations of the steady state grow if there are unstable wavenumbers $k \neq 0$, i.e. those for which $\Re(\sigma(k)) > 0$. Close inspection of the above reveals that this will hinge on the competition between stabilising (diffusion) and destabilising (aggregation) processes. In particular, the parameter regions in which self-organisation occur[q] are given by

$$\bar{u}\mu(R)R^2 > d \quad \text{and} \quad 2\bar{u}\nu(R)R > d \quad (5.4)$$

for the formulations (5.1) and (5.2), respectively. While phenomenologically similar, these two conditions are subtly distinct according to the relationships between the strength and range parameters.

Commonly, the nonlocal terms in models of type (1.2) are normalised, e.g. according to a measure of the size of the interaction space: in the context of (5.1) and (5.2), it is standard to choose $\mu(R) = \mu_0/2R$ and $\nu(R) = \nu_0/2R$. Under this choice, the instability conditions for the interaction strength (μ_0 or ν_0) and interaction range (R) have some clear distinctions for the two models (5.1) and (5.2)

---

[q]Note that this is under the infinite domain assumption, thereby allowing patterns to grow with unbounded wavelengths.
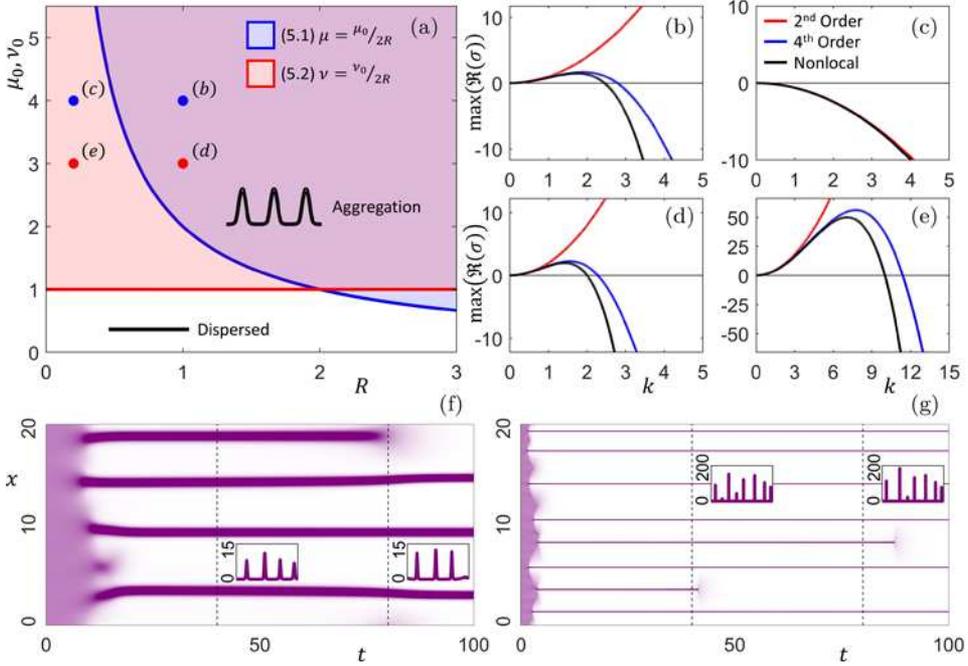
Fig. 6.   (Color online) (a) Parameter spaces for self-organisation as predicted by linear stability analysis, for (5.1) and (5.2) under $\mu(R) = \mu_0/2R$ and $\nu(R) = \nu_0/2R$, respectively. (b)–(e) Representative curves for the characteristic equations, corresponding to the points highlighted in (a): (b) and (c) formulation (5.1) and its second and fourth order approximations; (d) and (e) (5.2) and its second and fourth order approximations. (f) and (g) Simulations of (5.1) in 1D, for: (f) $(\alpha, R) = (1, 3)$; (g) $(\alpha, R) = (0.1, 21)$; density maps show the population density (white = low density, purple = density $\geq 4\bar{u}$), with inset figures showing the profile at the two times indicated by the dashed lines. For all plots, other parameters are set at $d = \bar{u} = 1$.

and become

$$\bar{u}\mu_0 R > 2d \quad \text{and} \quad \bar{u}\nu_0 > d, \quad \text{respectively.}$$

The condition for (5.2) is independent of R, while for (5.1) the capacity for self-organisation is lost as the interaction range decreases. We illustrate the parameter spaces in Fig. 6(a).

Characteristic equation curves for particular parameter values illustrate these behaviours: large R and sufficient μ_0 or ν_0 allow patterning for both models; correspondingly, a finite range of unstable wavenumbers is observed (Figs. 6(b) and 6(c), black curves). Decreasing R, the range of unstable wavenumbers either expands for (5.2) (Fig. 6(e)) or shrinks and disappears for (5.2) (Fig. 6(d)).

Further insights are obtained through expanding $u(x \pm y)$ inside (5.1) and (5.2) and truncating at different orders. The simplest nontrivial case (using $\mu = \mu_0/2R$, $\nu = \nu_0/2R$) leads to the second-order local approximations

$$\partial_t u = \partial_x \left[\left(d - \frac{\mu_0 R}{2} u \right) \partial_x u \right] \quad \text{and} \quad \partial_t u = \partial_x [(d - \nu_0 u)\partial_x u] \tag{5.5}$$

for (5.1) and (5.2), respectively. These immediately recall the density-dependent diffusion forms derived in Sec. 4.1.1. Instability regions for these equations are identical to those defined by (5.4), however this coincides with the region in which the models become illposed (negative diffusion); this manifests through corresponding characteristic equations whereby all wavenumbers are unstable, see red curves in Figs. 6(b)–6(e).

The expansions can also be truncated at higher order terms, and in particular the fourth order approximations become

$$\partial_t u = \partial_x \left[\left(d - \frac{\mu_0 R}{2} u \right) \partial_x u - \frac{\mu_0 R^3}{48} u \partial_{xxx} u \right] \tag{5.6}$$

and

$$\partial_t u = \partial_x \left[(d - \nu_0 u) \partial_x u - \frac{\nu_0 R^2}{6} u \partial_{xxx} \right] \tag{5.7}$$

for (5.1) and (5.2), respectively. Instability regions are again as those defined by (5.4). However, we now note that the destabilising second-order term is countered by a stabilising fourth-order term. The characteristic equations in this case generate finite ranges for unstable wavenumbers (blue curves, Figs. 6(b)–6(e)), curves closely following those of the nonlocal model (black curves). The distinct limiting behaviours as $R \to 0$ become clear from (5.6) and (5.7): the fourth order approximation to (5.1) implies convergence to a simple diffusion equation, with constant (and nonnegative) diffusion coefficient d; the fourth order approximation to (5.2), however, converges to a density-dependent form (second equation in (5.5)) with potential illposedness. We note that the fourth order approximations to nonlocal models have been studied in detail, e.g. in Ref. 183 for one variable models and in Ref. 71 for two variable models (see also Discussion and Challenges).

Stability analyses can, of course, be extended to explore pattern formation in multi-species models, for example those formulated to simulate adhesion-driven cell sorting. Scenarios under which pattern formation can occur will inevitably become more complicated within such models, as there are more potential routes to pattern formation (e.g. through the self interactions or through the cross interactions). We refer to Refs. 158 and 175 for examples of stability analyses for multi-species situations.

5.2. *Global existence and boundedness*

Our above observation of illposed local models that can follow from approximations of (1.2) leads to questions regarding the local and global existence of solutions: numerical solutions suggest that aggregates can become highly concentrated (e.g. Fig. 3(b)), but still appear to approach a bounded form. Does the presence of the nonlocal term lead to existence of solutions? This has formed a key point of inquiry for a number of publications (e.g. see Refs. 21, 50, 65, 72, 102, 124 and 184) related to (1.2).

For (1.2a), perhaps the most general theory[102] considers the following form of system:

$$\partial_t u = d\Delta u - \mu \nabla \cdot \left(u \int_{B_R(\mathbf{x})} f(u(\mathbf{x}+\mathbf{r},t)) \frac{\mathbf{r}}{|\mathbf{r}|} \omega(|\mathbf{r}|) d\mathbf{r} \right), \tag{5.8}$$

where $B_R(\mathbf{x})$ denotes the ball of radius $R > 0$ around $\mathbf{x}$.

Theorem 5.1. (Corollary 2.4 in Ref. 102) *Assume*

(A1) $f \in C^2(\mathbb{R}^n)$ *and there exists a value $b > 0$ such that $f(u) = 0$ for all $u \geq b$;*
(A2) $\omega \in L^1(\mathbb{R}^n)$, $\omega \geq 0$;
(A3) *for $p \geq 1$ let $u_0 \in X_p := C^0(\mathbb{R}^n) \cap L^\infty(\mathbb{R}^n) \cap L^p(\mathbb{R}^n)$ be nonnegative.*

Then there exists a unique, global solution

$$u \in C^0([0,\infty); X_p) \cap C^{2,1}(\mathbb{R}^n \times (0,\infty))$$

of (5.8) *in the classical sense, with $u(\mathbf{x},0) = u_0(\mathbf{x})$, $\mathbf{x} \in \mathbb{R}^n$.*

We remark that while the above immediately implies global existence of solutions in n-dimensions for a large class of formulations, it does not yet cover some standard choices. The oft-used formulation (2.2) is particularly delicate as, formally, (A1) states that f can only be linear up to a bounded density, but then becomes zero beyond some higher density. From the point of practical application this is sufficient, as we would naturally expect a bound to arise from physical or biological constraints, e.g. space limitations or saturation of receptors. Nevertheless, covering the case $f(u) = u$ without that explicit assumption remains an open problem.

The same Theorem 5.1 can also be used in the context of other aggregation models, and in particular we refer to the formulation based on energy minimisation, (1.3). To see this, we first note the connection of (5.8) to the energy-based formulation by supposing there exists some $W(|\mathbf{r}|)$ such that $\nabla W(|\mathbf{r}|) = \frac{\mathbf{r}}{|\mathbf{r}|}\omega(|\mathbf{r}|)$. Recalling that $\mathbf{r} = \mathbf{y} - \mathbf{x}$, straightforward calculations (shown in Appendix A) reveal that (5.8) can be rewritten as

$$\partial_t u = d\Delta u + \mu \nabla \cdot (u\nabla(W * f(u))). \tag{5.9}$$

Therefore, we can apply Theorem 5.1 directly.

Corollary 5.1. *Consider the model* (5.9) *where $\mu > 0$ and $W(|\mathbf{r}|)$ is a potential, a function of the distance of the interaction $|\mathbf{r}| = |\mathbf{y} - \mathbf{x}|$. Suppose f satisfies the same conditions as* (A.1), *the initial condition satisfies* (A.3) *and W satisfies*

(W1) $W(|\mathbf{r}|) \in L^\infty$, *and $W(|\mathbf{r}|)$ has compact support inside a ball $B_R(0)$.*
(W2) *There exists a scalar function $\omega(|\mathbf{r}|)$ such that $\nabla W(|\mathbf{r}|) = \frac{\mathbf{r}}{|\mathbf{r}|}\omega(|\mathbf{r}|)$ where $\omega(|\mathbf{r}|) \in L^1$ and $\omega(|\mathbf{r}|) \geq 0$.*

Then Eq. (5.9) *has a unique global classical solution*

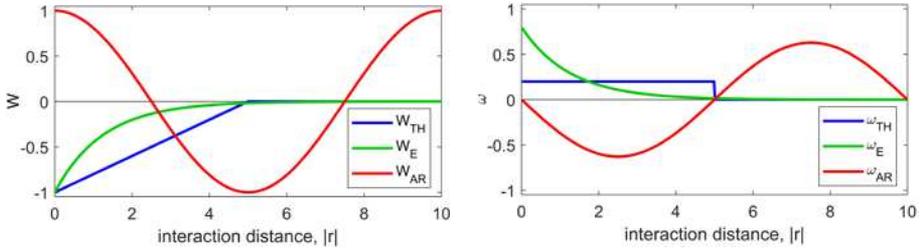$$u \in C^0([0,\infty); X_p) \cap C^{2,1}(\mathbb{R}^n \times (0,\infty)).$$

Fig. 7.   Examples of interaction potentials (left) and the corresponding forces (right), using $R = 5$. Here we consider the top hat potential W_{TH}, the exponential potential W_E, and the attraction–repulsion potential W_{AR}.

Proof. The proof follows immediately from Theorem 5.1 by replacing ∇W with $\frac{\mathbf{r}}{|\mathbf{r}|}\omega(|\mathbf{r}|)$.   □

Corollary 5.1 is the first existence result for aggregation models (1.2b) with general nonlinear response functions $f(u)$. However, the condition (W3) is quite restrictive. Since we require $\omega(|\mathbf{r}|) \geq 0$, condition (W2) imposes that the drift is always towards the origin, where the origin corresponds to the location of the probing individual. Hence the forces are always attractive. Examples of attractive potentials are shown in Fig. 7(a), and include the linear potential W_{TH} and the exponential potential (also called a Moore potential or Laplace kernel) W_E,

$$W_{\mathrm{TH}}(|\mathbf{r}|) = \min\left\{\frac{1}{R}|\mathbf{r}| - 1, 0\right\}, \quad W_E(|\mathbf{r}|) = -\exp\left(-\frac{4|\mathbf{r}|}{R}\right),$$

where R represents an interaction range parameter. The exponential kernel has unbounded support, but converges to zero quickly for larger $|\mathbf{r}|$; the factor of four ensures that this is close to zero for $|\mathbf{r}| = R$. Other purely attractive potentials include the Gaussian kernel and the Hegselman–Krause potential used in opinion dynamics (e.g. see Refs. 84, 95, 126 and 130).

In the cases described above the potential is strictly increasing for small values of $|\mathbf{r}|$, hence indicating an attractive force towards the origin. Indeed, the corresponding kernels $\omega(|\mathbf{r}|)$ are nonnegative (see Fig. 7(b)). As a point of note, under the linear potential W_{TH} we obtain a so-called top-hat kernel, e.g. as previously used in (2.2).

In the swarming literature it is quite common to consider potentials that describe both, attractive and repulsive effects. In such cases W is no longer monotonic, and hence ω changes sign: when W is increasing, $\omega > 0$, and we are in an attracting region; if W is decreasing, $\omega < 0$, and we are in a repelling region. One simple example of an attraction–repulsion potential, also shown in Fig. 7, is given by

$$W_{\mathrm{AR}}(|\mathbf{r}|) = \cos\left(\frac{\pi|\mathbf{r}|}{R}\right).$$

This stipulates a repelling region for interaction distances up to R, and an attracting region from R to $2R$. Note that the attraction–repulsion potential has a minimum at $|\mathbf{r}| = R$, at the point at which there is a switch from repulsion to attraction, and in this context R can be regarded as the preferred distance between individuals. Other examples of attractive and repulsive potentials are discussed in Ref. 43 and include the generalised Kuramoto model, the Onsager model for liquid crystals, and the Barré–Degond–Zatorska model.

5.3. *Bifurcation analysis*

There are two principal techniques that have been used to analyse bifurcations in models of the type in Eqs. (1.2) and (1.4): weakly nonlinear analysis (WNLA) and Crandall–Rabinowitz bifurcation theory (CRBT). Both techniques are useful for separating bifurcations into sub- and super-critical regimes. However, CRBT relies on steady-state formulations, whereas WNLA can reveal the criticality of bifurcations whereby the dominant eigenvalue is non-real and so solutions just beyond the bifurcation point oscillate in time. On the other hand CRBT can be used to understand the global nature of branches,[98] whereas WNLA is intrinsically local in its formulation.[134] We give examples here of both techniques, first CRBT then WNLA, applied to our models of interest, exemplifying valuable outcomes and important considerations when applying them.

5.3.1. *Crandall–Rabinowitz type bifurcation analysis*

Bifurcation analyses that use the Crandall and Rabinowitz framework[56, 178] (alongside methods from equivariant bifurcation theory[90]), have been carried out in a recent monograph.[98] To illustrate, we consider a particularly simple setting in one dimension, for the interval domain $[0, L]$ with a possibly nonlinear adhesion function $f(u)$:

$$\partial_t u = \partial_{xx} u - \mu \partial_x \left[u \int_{-1}^{1} f(u(x + r, t)) \frac{r}{|r|} \omega(|r|) dr \right], \tag{5.10}$$

where $\omega(|r|) \geq 0$, $\omega \in L^1(0,1) \cap L^\infty(0,1)$, and $\|\omega\|_{L^1(0,1)} = \frac{1}{2}$. In (5.10) we implicitly assume that the integral kernel has compact support in the interval $[-1, 1]$ and that $d = 1$, i.e. an assumed *a priori* rescaling of space and time that normalises the interaction range and diffusion coefficient to 1. Note that we set $L > 2$, such that the boundaries cannot be simultaneously touched. We equip $[0, L]$ with periodic boundary conditions

$$u(0, t) = u(L, t), \quad \partial_x u(0, t) = \partial_x u(L, t),$$

with the integral wrapped around in a natural way. The interaction strength parameter μ is taken as the bifurcation parameter.

We define the Fourier-sine coefficients of the sensing function ω as

$$M_n(\omega) = \int_0^1 \sin\left(\frac{2\pi n r}{L}\right) \omega(|r|) dr.$$

As the monograph[98] shows in detail, a number of properties can be identified for the following turning operator

$$K[u](x) = \int_{-1}^1 f(u(x+r,t)) \frac{r}{|r|} \omega(|r|) dr.$$

Specifically, K is found to be skew adjoint, $K[1] = 0$ and, for the specific case $f(u) = u$, maps sine and cosine functions as follows:

$$K\left[\sin\left(\frac{2\pi n x}{L}\right)\right] = 2M_n(\omega) \cos\left(\frac{2\pi n x}{L}\right),$$

$$K\left[\cos\left(\frac{2\pi n x}{L}\right)\right] = -2M_n(\omega) \sin\left(\frac{2\pi n x}{L}\right).$$

Moreover, if $u(x)$ is a steady state of (5.10), then $u'(x) = 0$ if and only if $K[u] = 0$, $u''(x) \leq 0$ implies $K'[u] \leq 0$, and $K'[u] \geq 0$ implies $u''(x) \geq 0$. In this context we can view $K[u]$ as a nonlocal derivative and $K'[u]$ as a nonlocal curvature of the solution.

The symmetries of $K[u]$ are also shown[98] to possess crucial properties. K has $O(2)$ symmetry and, as a consequence, bifurcation branches arise at discrete points through the following theorem.

Theorem 5.2. (See Ref. 98) *Consider a constant steady state $\bar{u}$ of (5.10) with $f'(\bar{u}) \neq 0$. For each $n = 1, 2, 3, \ldots$ with $M_n(\omega) > 0$ there exists a bifurcation value and eigenfunction as*

$$\mu_n = \frac{n\pi}{L\bar{u}f'(\bar{u})M_n(\omega)}, \quad e_n(x) = \cos\left(\frac{2\pi n x}{L}\right).$$

For a linear interaction function $f(u) = u$ it is also possible to identify the type of bifurcation via higher order expansions around the bifurcation value μ_n. Specifically, we arrive at the following theorem.

Theorem 5.3. (See Ref. 98) *If $f(u) = u$, then the type of bifurcation at μ_n is given by the sign of*

$$\beta_n = \frac{M_{2n}(\omega) - M_n(\omega)}{M_{2n}(\omega) - 2M_n(\omega)}.$$

If $\beta_n > 0$ then the bifurcation at μ_n is supercritical and for $\beta_n < 0$ it is subcritical.

Notably, the type of bifurcation turns out to be entirely determined by the Fourier sine modes of the sensing function $\omega(r)$.

Example. As an example, consider $f(u) = u$ and a top-hat kernel

$$\omega(r) = \frac{1}{2}\chi_{[-1,1]}(r).$$

Then the Fourier sine coefficients of ω are

$$M_n(\omega) = \frac{L}{2\pi n} \sin^2\left(\frac{n\pi}{L}\right),$$

and the bifurcation values are

$$\mu_n = \frac{2\pi^2 n^2}{L^2 \bar{u} \sin^2\left(\frac{n\pi}{L}\right)}.$$

If L is a multiple of π, certain bifurcation values do not exist. Otherwise, all μ_n are well defined. The type of bifurcation is given by the sign of

$$\beta_n = 2\left(1 - \cot^2\left(\frac{n\pi}{L}\right)\right),$$

which, indeed, can be positive or negative.

As in the previous subsection, a close relationship can be observed between model (5.10) and those formulated from an energy based approach. Given the sensing function $\omega(r)$, we define a potential

$$W(r) := V(r)\chi_{[-1,1]}(r) \quad \text{with } V'(r) = \omega(r). \tag{5.11}$$

Then for smooth solutions model (5.10) is equivalent with

$$\partial_t u = \partial_{xx} u + \mu \partial_x [u \partial_x (W * f(u))]. \tag{5.12}$$

As such, the bifurcation result of Theorem 5.2 can be extended to this case.

Corollary 5.2. *Consider* (5.12) *where the potential is given by* (5.11). *Then, for each* $n = 1, 2, 3, \ldots$ *with* $M_n(\omega) > 0$, *there exists a bifurcation value and eigenfunction given by*

$$\mu_n = \frac{n\pi}{L\bar{u}f'(\bar{u})M_n(\omega)}, \quad e_n(x) = \cos\left(\frac{2\pi n x}{L}\right).$$

As a point of remark, in Ref. 43 the bifurcations of (5.12) were considered only for the linear case $f(u) = u$. For that case, the bifurcation value at equilibrium $\bar{u} = \frac{1}{L}$ was expressed as

$$\mu_n^* = -\frac{(2L)^{1/2}}{\tilde{W}(n)},$$

where

$$\tilde{W}(n) = \sqrt{\frac{2}{L}} \int_0^L W(x) \cos\left(\frac{2\pi k x}{L}\right) dx$$

denotes the Fourier cosine coefficient of the potential W. We can directly compute that

$$\tilde{W}(n) = -\frac{\sqrt{2L}}{\pi n} M_n(\omega),$$

which implies $\mu_n = \mu_n^*$: a satisfying confirmation of our results. Note that in Ref. 43 bifurcation analysis was also extended to arbitrary space dimensions, exceeding what has currently been performed for formulations of type (1.2a).

5.3.2. *Weakly nonlinear analysis and conservation laws*

We observed above that bifurcations emerge at well-defined strictly positive wavenumbers, which is a rather typical behaviour for many reaction–diffusion systems.[150] In most cases, weakly nonlinear analysis (WNLA) can be used to reveal a Stuart–Landau equation governing the amplitude of the patterns close to the bifurcation point. However, when the PDE possesses a conservation law, i.e. $\frac{\mathrm{d}}{\mathrm{d}t} \int_\Omega u \mathrm{d}x = 0$, the situation is rather more complicated. In particular, the wavenumber that is destabilised first can be arbitrarily close to the origin, often meaning that the Stuart–Landau formalism is insufficient for capturing the dynamics of the amplitude of patterns.[59, 134] Such a situation is pertinent here, as Eqs. (1.2) and (1.4) can all possess conservation laws under certain boundary conditions (e.g. periodic).

To explain this in more detail, it is valuable to look at a specific example. To this end, we consider a recently studied symmetric 2-species version of Eq. (1.4) given by[86]

$$\partial_t u_1 = \partial_{xx} u_1 + \gamma \partial_x (u_1 \partial_x (K * u_2)),$$
$$\partial_t u_2 = \partial_{xx} u_2 + \gamma \partial_x (u_2 \partial_x (K * u_1)),$$
(5.13)

defined on $x \in [-\frac{L}{2}, \frac{L}{2}]$ for $L > 2$, with $\mathrm{Supp}(K) = [-1, 1]$ and periodic boundary conditions. Let $\bar{\mathbf{u}} = (\bar{u}_1, \bar{u}_2)$ be the constant steady state. In the case $\gamma > 0$, we can think of this as modelling two mutually avoiding populations with identical advective and diffusive properties, for example territorial groups of animals. For $\gamma < 0$, this models mutually-attractive populations, for example symbiotic animal species, or cell-types that have mutual adhesive tendencies.

As is standard in WNLA, the authors of Ref. 86 first decompose space and time into short and long scales. Specifically, they define $X = \epsilon x$ and $T = \epsilon^2 t$. Then they look for solutions of the form[134]

$$\mathbf{u}(x, t) = \bar{\mathbf{u}} + A(X, T)e^{iq_c x} + A^*(X, T)e^{-iq_c x} + B(X, T),$$
(5.14)

where q_c is the first wavenumber to be destabilised as γ passes through the bifurcation threshold. In situations where there is no conservation law, and the zero mode is stable close to the bifurcation point, there is no need to include the term $B(X, T)$. However, the conservation law means that the zero mode always has an eigenvalue of zero so can be unstable to spatial perturbations on the slow-time, long-space scale (i.e. in (X, T) coordinates). It should be noted that the amplitudes A and B depend on the macroscopic time and space scales, while the mode $e^{iq_c x}$ depends on the microscale. In particular, the authors showed[86] that if $\bar{u}_1 \neq \bar{u}_2$, A is governed

by the Stuart–Landau equation

$$A_T = q_c^2 A - \Lambda |A|^2 A, \tag{5.15}$$

and $B = 0$, whenever γ is in the linearly unstable regime. However, if $\bar{u}_1 = \bar{u}_2$ then there is a different system of amplitude equations

$$A_T = q_c^2 A - \Lambda |A|^2 A + \frac{q_c^2}{\bar{u}_1} AB, \tag{5.16}$$

$$B_T = \eta B_{XX} - \frac{1}{\bar{u}_1} (|A|^2)_{XX}, \tag{5.17}$$

where η is a function of γ_c, $\bar{u}_1$ and $\hat{K}(0)$, where $\hat{K}(q)$ is the Fourier-cosine coefficient of $K(x)$

$$\hat{K}(q) = \int_{-1}^{1} K(x) \cos(qx) \mathrm{d}x. \tag{5.18}$$

In Eqs. (5.15) and (5.16), Λ controls the criticality of the bifurcation in A, and is a function of $\hat{K}(q_c)$, $\hat{K}(2q_c)$, $\bar{u}_1$, $\bar{u}_2$ and γ_c (see Ref. 86 for precise functional forms of Λ and η). In the $\bar{u}_1 = \bar{u}_2$ case, due to the contribution of the function $B(X, T)$, branches that bifurcate supercritically in $A(X, T)$ can be unstable. Indeed, the following proposition holds.

Proposition 5.1. *Suppose $\bar{u}_1 = \bar{u}_2$. If γ is in the linearly unstable regime and $\Lambda > 0$ then small amplitude patterns to System (5.13) exist. These solutions are unstable if*

$$\Lambda < \frac{\bar{u}_1^2}{q_c^2 \eta}. \tag{5.19}$$

This means that, in the case $0 < \Lambda < \frac{\bar{u}_1^2}{q_c^2 \eta}$, we have a supercritical bifurcation, but unlike the Stuart–Landau situation, stable patterns do not grow continuously as the bifurcation point is crossed. Rather, numerical solutions show a discontinuous jump to a higher amplitude than the supercritical branch predicts.[86] This case study shows the importance of accounting for the zero mode in bifurcation analysis of nonlocal advection–diffusion equations. Whilst we have only shown this in a single example, it is reasonable to expect that unstable supercritical branches may be a phenomenon observed more generally.

6. Discussion and Challenges

To conclude, we outline a number of outstanding issues regarding modelling with nonlocal advection, and provide a few potential ways forward that could be fruitful in the coming years.

Existence results. A large existence theory has been developed, which covers a relatively broad spectrum of models that lie in the forms (1.2)–(1.4). However, the

generalised structure of these equations can lead to a vast spectrum of models and an all-encompassing theory is not yet available. For example, functions $\mathbf{k}$ (or w) can vary from positive to negative and systems with multiple species can admit a wide spectrum of cross interactions.

Steady states, stability and bifurcation structure. Dynamically, models (1.2)–(1.4) are capable of an extremely rich variety of patterning, including stationary aggregate patterns, oscillating structures, travelling wave dynamics. Classical Turing-type stability analyses of nonlocal models have generally focused on one spatial dimension; intriguingly, however, recent extensions[110] to higher dimensions indicate a dimensionally-dependent self-organising capacity, with patterning possible in higher dimensions for a formulation incapable of self-organisation in one-dimension. Studies into long time behaviours have primarily relied on simulations, however this alone is far from satisfactory: transients can persist over long timescales and become confused with stationary solutions. As an example, referring to Figs. 6(f) and 6(g), a coarsening sequence is observed in which aggregates collapse over time: is the long time outcome a single aggregate? Expanding analytical methods, such as energy functional approaches,[47, 85] would have high value in generating a more nuanced understanding into steady states and bifurcation structures.

Boundary effects. In a nonlocal model, individuals inside some domain Ω may conceivably sense information from outside Ω. The act of writing the nonlocal term at or close to a boundary therefore requires thought, as its support may extend beyond the domain of definition of the model. One can sidestep this through wrapping the nonlocal term around the domain, via the imposition of periodic boundary conditions.[84] Another approach is to alter the definition of the nonlocal term, in a mathematically consistent way, as it approaches the boundary.[97] More broadly, the potential range of boundary conditions is immense and requires consideration on an application-to-application basis. For example, for adhesive populations one could allow the external space to exert varying levels of 'stickiness', or be actively repelling, according to tissue structure; in the case of multiple populations, different populations may respond distinctly near the interface. Non-standard boundary conditions can strongly influence patterning within classical models (e.g. for reaction diffusion systems see Refs. 63 and 168), and it is natural to expect a similarly powerful impact of boundary conditions on the aggregation models considered here.

Local formulations. Widescale adoption of nonlocal models is hindered by the analytical and numerical challenges. While efficient numerical methods have been developed — Fast Fourier Transforms for the integral calculation,[80] positivity preserving finite volume methods,[44] pseudospectral methods[89] — formulating local models with similar properties could assist both numerics and analysis. As noted, second-order local models can be derived from random walk models[6, 111] and formal analyses[67] have investigated convergence between local and nonlocal forms. However, the potential of illposed local forms remains an issue. Fourth order local

equations provide a promising avenue, and in Ref. 71 the following two species local
model for sorting was derived from an underlying nonlocal system:

$$\partial_t u = -\nabla \cdot [u\nabla(\mu\Delta u + \beta\Delta v + \gamma u + \delta v)],$$

$$\partial_t v = -\nabla \cdot [v\nabla(\beta\Delta u + \Delta v + \delta u + v)].$$

The parameters in the above relate to those in the nonlocal interaction terms and
the above model was shown to be capable of reproducing a similar range of sorting
dynamics to those of nonlocal models. Overall, derivation and exploration of well
behaved local models is of importance.

Structured populations. Population heterogeneity in nonlocal models is typ-
ically restricted to two state systems, i.e. two populations with distinct proper-
ties. Discretisation into distinct subpopulations is often an approximation within
biological systems: for example, studies[123] of invasive breast cancer cells indicate
invading cells lie on a continuum of intermediate states from epithelial to mesenchy-
mal; individual-to-individual variation of 'animal personality'[115, 166, 212] plays an
important role in collective animal movements. Instead of extending the number
of subpopulations in (1.4), subtle variation could be treated through a structured
population framework: extending to a density $u(\mathbf{x}, p, t)$ where p represents the phe-
notype state, and choosing interaction terms to describe how different phenotypes
influence the dynamics.[165]

Applications to sociological systems. This review has concentrated on nonlocal
PDEs motivated by biological systems, in particular the spatiotemporal structuring
of animals and cells. Naturally, the models and methods have applications beyond
those areas, in particular to sociological systems. Perhaps the most germane exam-
ple here would be crowds and traffic. This is an area that has witnessed much
modelling with techniques ranging from agent-based to continuous (e.g. see Refs. 16
and 91) and frameworks developed to scale between such models (e.g. see Ref. 15)
have the potential to be adapted to the systems considered here. Concepts of stig-
mergy also cross to social systems, for example gang territoriality where agent-based
modelling[13] has shown that territories can emerge indirectly through graffiti rather
than direct conflict. Nonlocal models directly related to Eq. (1.2a) have been derived
from agent-based models in the context of opinion dynamics (e.g. see Refs. 11, 78, 89
and 167), where movement through physical space becomes a movement across
opinion space and aggregation corresponds to consensus. Undoubtedly, numerous
sociological problems may benefit from the frameworks considered here.

Testing predictions. Mathematical modelling of biological pattern formation is
often inspired by the attempt to understand patterns already observed in biological
systems: as examples, here we have described nonlocal models formulated to repro-
duce the observed patterns from cell sorting or territory formation. However, one
can also use models to predict patterns that could be observed. For example, the
multi-species equations (1.4) display rich pattern formation properties that ought

to be observable in natural systems, if the models contain a sufficiently accurate representation of the underlying interactions. Patterns emerging from the model that have not yet been identified in the real world can be viewed as predictions: do these patterns actually emerge in distributions if movement data is collected and/or analysed appropriately? If so, this would lead to new knowledge on the variety of patterns that can form spontaneously in populations of moving organisms. If not, this would inform us of missing features in our models, and deepen our understanding of the drivers of organism space use.

Connecting to data. Testing predictions demands techniques for connecting models and data. Beyond those reported here, as a further example, machine learning algorithms (e.g. see Ref. 129) allow trajectory data to be translated into interaction kernels for ABMs, which can then be scaled to PDEs. However, deciding the most appropriate for the data and question at hand is far from straightforward. To give an example from animal ecology, there are broadly two classes of techniques for fitting PDE models to data that are currently applied. The first starts by building a PDE model based on qualitative aspects of behaviour that have been observed. Then the emergent patterns from numerical solutions of the PDE model are fitted to location data, to uncover the underlying behavioural processes in a more quantitative way. This is exemplified in studies of mechanistic home range analysis.[144] The second approach follows that described in Sec. 4.1.3, where a movement kernel (a.k.a. position jump process) like in Eq. (4.9) is fitted to a time series of location data. Then the PDE model is derived from this movement kernel.[170] The comparison between emergent pattern in the model and in the data then serves as a kind of 'goodness-of-fit' test for the model, which can serve to uncover missing covariates of animal movement decisions.[171] Whilst this contrast in techniques has been known in the literature for some time,[172] these two approaches could do with some unification to achieve the maximum scientific benefit from analysing a given dataset.

Collective cell movement. The analysis of collective cell movement forms a highly active area of research, from embryonic development to cancer invasion processes (e.g. see Refs. 135 and 218), and a large number of modelling approaches have been developed (e.g. Refs. 4 and 37). Often, migrating cells extend long thin protrusions into their environment, possibly conferring an element of nonlocal sensing: for example, the formation of numerous lengthy filopodia appears to play an important role during effective migration of neural crest cells,[136] while long thin 'tumor microtubes' play an apparently crucial role by facilitating invasion and growth of certain brain tumors (e.g. Refs. 99 and 154). Mathematical analysis of models capable of incorporating potential nonlocal impacts, as discussed here, promise new biological insight.

The growth of mathematical biology in recent decades has been spectacular, crossing scales and disciplines. However, the trade off is fragmentation: mathematical ecology, mathematical oncology etc. form their own fields, collaborative

networks have become specialised, and keeping pace with developments in other fields becomes a challenge. Despite this, the common language of mathematics remains. A key aim of this review has been to demonstrate this, showing the connection between nonlocal models used in ecological and cellular systems and suggesting the two fields can mutually benefit from their ongoing developments.

Appendix A. Correspondence Between Models

We demonstrate the calculations that show the translation between (5.8) and (5.9). Specifically, we assume there exists a potential $W(|\mathbf{r}|)$ such that

$$\nabla_{\mathbf{r}} W(|\mathbf{r}|) = \frac{\mathbf{r}}{|\mathbf{r}|} \omega(|\mathbf{r}|). \tag{A.1}$$

Substituting (A.1) into (5.8) and noting

$$\mathbf{y} = \mathbf{x} + \mathbf{r}, \quad \mathbf{r} = \mathbf{y} - \mathbf{x}, \quad d\mathbf{y} = d\mathbf{r}, \quad \nabla_{\mathbf{y}} = \nabla_{\mathbf{r}},$$

$$u_t = d\Delta u - \mu \nabla \left(u \int_{B_R(x)} f(u(\mathbf{x} + \mathbf{r})) \nabla_{\mathbf{r}} W(|\mathbf{r}|) d\mathbf{r} \right)$$

$$= d\Delta u - \mu \nabla \left(u \int_{B_R(0)} f(u(\mathbf{y})) \nabla_{\mathbf{y}} W(|\mathbf{y} - \mathbf{x}|) d\mathbf{y} \right)$$

$$= d\Delta u + \mu \nabla \left(u \int_{B_R(0)} f(u(\mathbf{y})) \nabla_{\mathbf{x}} W(|\mathbf{y} - \mathbf{x}|) d\mathbf{y} \right)$$

$$= d\Delta u + \mu \nabla (u(\nabla_{\mathbf{x}} W) * f(u))$$

$$= d\Delta u + \mu \nabla (u \nabla (W * f(u))).$$

The above shows that energy minimisation corresponds to attractive interactions between individuals. Note that where subscripts are not included $\nabla \equiv \nabla_{\mathbf{x}}$ and $\Delta \equiv \Delta_{\mathbf{x}}$.

Acknowledgments

ORCID

Kevin J. Painter ● https://orcid.org/0000-0003-3273-6031

Thomas Hillen ⬤ https://orcid.org/0000-0003-0819-9520

Jonathan R. Potts ⬤ https://orcid.org/0000-0002-8564-2904

References

1. M. Abercrombie and J. E. Heaysman, Observations on the social behaviour of cells in tissue culture: II. "Monolayering" of fibroblasts, *Exp. Cell Res.* **6** (1954) 293–306.
2. E. S. Adams, Approaches to the study of territory size and shape, *Annu. Rev. Ecol. Syst.* **32** (2001) 277–303.
3. B. Alberts, A. Johnson, J. Lewis, D. Morgan, M. Raff, K. Roberts and P. Walter, *Molecular Biology of the Cell*, 6th edn. (Taylor & Francis Group, 2015).
4. R. Alert and X. Trepat, Physical models of collective cell migration, *Annu. Rev. Condens. Matter Phys.* **11** (2020) 77–101.
5. J. D. Amack and M. L. Manning, Knowing the boundaries: Extending the differential adhesion hypothesis in embryonic cell sorting, *Science* **338** (2012) 212–215.
6. K. Anguige and C. Schmeiser, A one-dimensional model of cell diffusion and aggregation, incorporating volume filling and cell-to-cell adhesion, *J. Math. Biol.* **58** (2009) 395–427.
7. I. Aoki, A simulation study on the schooling mechanism in fish, *Bull. Jpn. Soc. Sci. Fish.* **48** (1982) 1081–1088.
8. N. J. Armstrong, K. J. Painter and J. A. Sherratt, A continuum approach to modelling cell–cell adhesion, *J. Theor. Biol.* **243** (2006) 98–113.
9. N. J. Armstrong, K. J. Painter and J. A. Sherratt, Adding adhesion to a chemical signaling model for somite formation, *Bull. Math. Biol.* **71** (2009) 1–24.
10. T. Avgar, J. R. Potts, M. A. Lewis and M. S. Boyce, Integrated step selection analysis: Bridging the gap between resource selection and animal movement, *Methods Ecol. Evol.* **7** (2016) 619–630.
11. P. Balenzuela, J. P. Pinasco and V. Semeshenko, The undecided have the key: Interaction-driven opinion dynamics in a three state model, *PLoS One* **10** (2015) e0139572.
12. M. Ballerini *et al.*, Empirical investigation of starling flocks: A benchmark study in collective animal behaviour, *Anim. Behav.* **76** (2008) 201–215.
13. A. B. Barbaro, L. Chayes and M. R. D'Orsogna, Territorial developments based on graffiti: A statistical mechanics approach, *Phys. A*: *Stat. Mech. Appl.* **392** (2013) 252–270.
14. G. Bastille-Rousseau, D. L. Murray, J. A. Schaefer, M. A. Lewis, S. P. Mahoney and J. R. Potts, Spatial scales of habitat selection decisions: Implications for telemetry-based movement modelling, *Ecography* **41** (2018) 437–443.
15. N. Bellomo, L. Gibelli, A. Quaini and A. Reali, Towards a mathematical theory of behavioral human crowds, *Math. Models Methods in Appl. Sci.* **32** (2022) 321–358.
16. N. Bellomo, J. Liao, A. Quaini, L. Russo and C. Siettos, Human behavioral crowds: Review, critical analysis, and research perspectives, *Math. Models Methods Appl. Sci.* **33** (2023) 1611–1659.
17. N. Bellomo, N. Outada, J. Soler, Y. Tao and M. Winkler, Chemotaxis and cross-diffusion models in complex environments: Models and analytic problems toward a multiscale vision, *Math. Models Methods Appl. Sci.* **32** (2022) 713–792.
18. A. M. Berdahl, A. B. Kao, A. Flack, P. A. Westley, E. A. Codling, I. D. Couzin, A. I. Dell and D. Biro, Collective animal navigation and migratory culture: From theoretical models to empirical evidence, *Philos. Trans. R. Soc. B*: *Biol. Sci.* **373** (2018) 20170009.

19. H. C. Berg, *Random Walks in Biology* (Princeton Univ. Press, 1993).

20. S. Bernardi, R. Eftimie and K. J. Painter, Leadership through influence: what mechanisms allow leaders to steer a swarm? *Bull. Math. Biol.* **83** (2021) 69.

21. A. L. Bertozzi and D. Slepcev, Existence and uniqueness of solutions to an aggregation equation with degenerate diffusion, *Commun. Pure Appl. Anal.* **9** (2010) 1617–1637.

22. H. L. Beyer, E. Gurarie, L. Börger, M. Panzacchi, M. Basille, I. Herfindal, B. Van Moorter, S. R. Lele and J. Matthiopoulos, 'you shall not pass!': Quantifying barrier permeability and proximity avoidance by animals, *J. Anim. Ecol.* **85** (2016) 43–53.

23. R. Bhat, T. Glimm, M. Linde-Medina, C. Cui and S. A. Newman, Synchronization of hes1 oscillations coordinates and refines condensation formation and patterning of the avian limb skeleton, *Mech. Dev.* **156** (2019) 41–54.

24. V. Bitsouni, M. A. Chaplain and R. Eftimie, Mathematical modelling of cancer invasion: The multiple roles of TGF-β pathway on tumour proliferation and cell adhesion, *Math. Models Methods Appl. Sci.* **27** (2017) 1929–1962.

25. V. Bitsouni, D. Trucu, M. A. Chaplain and R. Eftimie, Aggregation and travelling wave dynamics in a two-population model of cancer cell growth and invasion, *Math. Med. Biol.* **35** (2018) 541–577.

26. J. T. Bonner, *The Social Amoebae*: *The Biology of Cellular Slime Molds* (Princeton Univ. Press, 2009).

27. L. Börger, B. D. Dalziel and J. M. Fryxell, Are there general mechanisms of animal home range behaviour? A review and prospects for future research, *Ecol. Lett.* **11** (2008) 637–650.

28. B. K. Briscoe, M. A. Lewis and S. E. Parrish, Home range formation in wolves due to scent marking, *Bull. Math. Biol.* **64** (2002) 261–284.

29. G. W. Brodland, The differential interfacial tension hypothesis (DITH): A comprehensive theory for the self-rearrangement of embryonic cells and tissues, *J. Biomech. Eng.* **124** (2002) 188–197.

30. E. O. Budrene and H. C. Berg, Complex patterns formed by motile cells of *Escherichia coli*, *Nature* **349** (1991) 630–633.

31. E. O. Budrene and H. C. Berg, Dynamics of formation of symmetrical patterns by chemotactic bacteria, *Nature* **376** (1995) 49–53.

32. P.-L. Buono and R. Eftimie, Symmetries and pattern formation in hyperbolic versus parabolic models of self-organised aggregation, *J. Math. Biol.* **71** (2015) 847–881.

33. M. Burger, V. Capasso and D. Morale, On an aggregation model with long and short range interactions, *Nonlinear Anal.*: *Real World Appl.* **8** (2007) 939–958.

34. M. Burger, M. D. Francesco, S. Fagioli and A. Stevens, Sorting phenomena in a mathematical model for two mutually attracting/repelling species, *SIAM J. Math. Anal.* **50** (2018) 3210–3250.

35. W. H. Burt, Territoriality and home range concepts as applied to mammals, *J. Mammal.* **24** (1943) 346–352.

36. J. O. Bush, Cellular and molecular mechanisms of eph/ephrin signaling in evolution and development, *Curr. Top. Dev. Biol.* **149** (2022) 153–201.

37. A. Buttenschön and L. Edelstein-Keshet, Bridging from single to collective cell migration: A review of models and links to experiments, *PLoS Comput. Biol.* **16** (2020) e1008411.

38. A. Buttenschön, T. Hillen, A. Gerisch and K. J. Painter, A space-jump derivation for non-local models of cell–cell adhesion and non-local chemotaxis, *J. Math. Biol.* **76** (2018) 429–456.

39. H. Byrne, The importance of intercellular adhesion in the development of carcinomas, *Math. Med. Biol.* **14** (1997) 305–323.

40. H. M. Byrne and M. A. Chaplain, Modelling the role of cell–cell adhesion in the growth and development of carcinomas, *Math. Comput. Modell.* **24** (1996) 1–17.

41. C. Carmona-Fontaine, H. K. Matthews, S. Kuriyama, M. Moreno, G. A. Dunn, M. Parsons, C. D. Stern and R. Mayor, Contact inhibition of locomotion *in vivo* controls neural crest directional migration, *Nature* **456** (2008) 957–961.

42. J. Carrillo, Y. Choi and M. Hauray, The derivation of swarming models: Mean filed limit and Wasserstein distances, in *Collective Dynamics from Bacteria to Crowds* (Springer, 2014), pp. 1–46.

43. J. Carrillo, R. Galvani, G. Pavliotis and A. Schlichting, Long-time behavior and phase transitions for the McKean–Vlasov equation on a torus, *Arch. Ration. Mech. Anal.* **235** (2020) 635–690.

44. J. A. Carrillo, A. Chertock and Y. Huang, A finite-volume method for nonlinear non-local equations with a gradient flow structure, *Commun. Comput. Phys.* **17** (2015) 233–258.

45. J. A. Carrillo, A. Colombi and M. Scianna, Adhesion and volume constraints via nonlocal interactions determine cell organisation and migration profiles, *J. Theor. Biol.* **445** (2018) 75–91.

46. J. A. Carrillo, M. Fornasier, G. Toscani and F. Vecil, Particle, kinetic, and hydro-dynamic models of swarming, in *Mathematical Modeling of Collective Behavior in Socio-Economic and Life Sciences* (Springer, 2010), pp. 297–336.

47. J. A. Carrillo and R. S. Gvalani, Phase transitions for nonlinear nonlocal aggregation–diffusion equations, *Commun. Math. Phys.* **382** (2021) 485–545.

48. J. A. Carrillo, Y. Huang and M. Schmidtchen, Zoology of a nonlocal cross-diffusion model for two species, *SIAM J. Appl. Math.* **78** (2018) 1078–1104.

49. J. A. Carrillo, H. Murakawa, M. Sato, H. Togashi and O. Trush, A population dynamics model of cell–cell adhesion incorporating population pressure and density saturation, *J. Theor. Biol.* **474** (2019) 14–24.

50. M. A. Chaplain, M. Lachowicz, Z. Szymańska and D. Wrzosek, Mathematical mod-elling of cancer invasion: The importance of cell–cell adhesion and cell–matrix adhe-sion, *Math. Models Methods Appl. Sci.* **21** (2011) 719–743.

51. L. Chen, K. Painter, C. Surulescu and A. Zhigun, Mathematical models for cell migration: A non-local perspective, *Philos. Trans. R. Soc. B* **375** (2020) 20190379.

52. D. Chodniewicz and R. L. Klemke, Guiding cell migration through directed extension and stabilization of pseudopodia, *Exp. Cell Res.* **301** (2004) 31–37.

53. E. A. Codling, M. J. Plank and S. Benhamou, Random walk models in biology, *J. R. Soc. Interface* **5** (2008) 813–834.

54. I. D. Couzin, J. Krause, N. R. Franks and S. A. Levin, Effective leadership and decision-making in animal groups on the move, *Nature* **433** (2005) 513–516.

55. I. D. Couzin, J. Krause, R. James, G. D. Ruxton and N. R. Franks, Collective memory and spatial sorting in animal groups, *J. Theor. Biol.* **218** (2002) 1–11.

56. M. Crandall and P. Rabinowitz, Bifurcation from simple eigenvalues, *J. Funct. Anal.* **8** (1971) 321–340.

57. V. Cristini, X. Li, J. S. Lowengrub and S. M. Wise, Nonlinear simulations of solid tumor growth using a mixture model: Invasion and branching, *J. Math. Biol.* **58** (2009) 723–763.

58. V. Cristini, J. Lowengrub and Q. Nie, Nonlinear simulation of tumor growth, *J. Math. Biol.* **46** (2003) 191–224.

59. M. C. Cross and P. C. Hohenberg, Pattern formation outside of equilibrium, *Rev. Mod. Phys.* **65** (1993) 851.

60. F. Cucker and S. Smale, Emergent behavior in flocks, *IEEE Trans. Autom. Control* **52** (2007) 852–862.

61. A. Deutsch and S. Dormann, *Cellular Automaton Modeling of Biological Pattern Formation*, Modeling and Simulation in Science, Engineering and Technology (Birkhäuser, 2005).

62. M. Di Francesco and S. Fagioli, A nonlocal swarm model for predators–prey interactions, *Math. Models Methods Appl. Sci.* **26** (2016) 319–355.

63. R. Dillon, P. Maini and H. Othmer, Pattern formation in generalized turing systems: I. Steady-state patterns in systems with mixed boundary conditions, *J. Math. Biol.* **32** (1994) 345–393.

64. P. Domschke, D. Trucu, A. Gerisch and M. A. Chaplain, Mathematical modelling of cancer invasion: Implications of cell adhesion variability for tumour infiltrative growth patterns, *J. Theor. Biol.* **361** (2014) 41–60.

65. J. Dyson, S. A. Gourley, R. Villella-Bressan and G. F. Webb, Existence and asymptotic properties of solutions of a nonlocal evolution equation modeling cell–cell adhesion, *SIAM J. Math. Anal.* **42** (2010) 1784–1804.

66. J. Dyson, S. A. Gourley and G. F. Webb, A non-local evolution equation model of cell–cell adhesion in higher dimensional space, *J. Biol. Dyn.* **7** (2013) 68–87.

67. M. Eckardt, K. J. Painter, C. Surulescu and A. Zhigun, Nonlocal and local models for taxis in cell migration: A rigorous limit procedure, *J. Math. Biol.* **81** (2020) 1251–1298.

68. R. Eftimie, *Hyperbolic and Kinetic Models for Self-organised Biological Aggregations* (Springer, 2018).

69. R. Eftimie, G. de Vries and M. A. Lewis, Complex spatial group patterns result from different animal communication mechanisms, *Proc. Natl. Acad. Sci.* **104** (2007) 6974–6979.

70. W. F. Fagan, T. Hoffman, D. Dahiya, E. Gurarie, R. S. Cantrell and C. Cosner, Improved foraging by switching between diffusion and advection: Benefits from movement that depends on spatial context, *Theor. Ecol.* **13** (2020) 127–136.

71. C. Falcó, R. E. Baker and J. A. Carrillo, A local continuum model of cell–cell adhesion, *SIAM J. Appl. Math.* (2023) S17–S42.

72. R. C. Fetecau, Y. Huang and T. Kolokolnikov, Swarm dynamics and equilibria for a nonlocal aggregation model, *Nonlinearity* **24** (2011) 2681.

73. J. Fieberg, J. Signer, B. Smith and T. Avgar, A 'how to' guide for interpreting parameters in habitat-selection analyses, *J. Anim. Ecol.* **90** (2021) 1027–1043.

74. A. G. Fletcher, M. Osterfield, R. E. Baker and S. Y. Shvartsman, Vertex models of epithelial morphogenesis, *Biophys. J.* **106** (2014) 2291–2304.

75. J. D. Forester, H. K. Im and P. J. Rathouz, Accounting for animal movement in estimation of resource selection functions: Sampling and data analysis, *Ecology* **90** (2009) 3554–3565.

76. D. Fortin, H. L. Beyer, M. S. Boyce, D. W. Smith, T. Duchesne and J. S. Mao, Wolves influence elk movements: Behavior shapes a trophic cascade in Yellowstone National Park, *Ecology* **86** (2005) 1320–1330.

77. R. A. Foty and M. S. Steinberg, The differential adhesion hypothesis: A direct evaluation, *Dev. Biol.* **278** (2005) 255–263.

78. J. Garnier, G. Papanicolaou and T.-W. Yang, Consensus convergence with stochastic effects, *Vietnam J. Math.* **45** (2017) 51–75.

79. F. Georgiou, J. Buhl, J. Green, B. Lamichhane and N. Thamwattana, Modelling locust foraging: How and why food affects group formation, *PLoS Comput. Biol.* **17** (2021) e1008353.

80. A. Gerisch, On the approximation and efficient evaluation of integral terms in PDE models of cell adhesion, *IMA J. Numer. Anal.* **30** (2010) 173–194.

81. A. Gerisch and M. A. Chaplain, Mathematical modelling of cancer cell invasion of tissue: Local and non-local models and the effect of adhesion, *J. Theor. Biol.* **250** (2008) 684–704.

82. A. Gerisch and K. J. Painter, Mathematical modeling of cell adhesion and its applications to developmental biology and cancer invasion, in *Cell Mechanics* (Chapman and Hall/CRC, 2010), pp. 337–368.

83. A. Ghaffarizadeh, R. Heiland, S. H. Friedman, S. M. Mumenthaler and P. Macklin, Physicell: An open source physics-based cell simulator for 3-d multicellular systems, *PLoS Comput. Biol.* **14** (2018) e1005991.

84. V. Giunta, T. Hillen, M. Lewis and J. R. Potts, Local and global existence for nonlocal multispecies advection–diffusion models, *SIAM J. Appl. Dyn. Syst.* **21** (2022) 1686–1708.

85. V. Giunta, T. Hillen, M. A. Lewis and J. R. Potts, Detecting minimum energy states and multi-stability in nonlocal advection–diffusion models for interacting species, *J. Math. Biol.* **85** (2022) 1–44.

86. V. Giunta, T. Hillen, M. A. Lewis and J. R. Potts, Weakly nonlinear analysis of a two-species non-local advection–diffusion system, preprint (2023), arXiv:2305.14954.

87. J. A. Glazier and F. Graner, Simulation of the differential adhesion driven rearrangement of biological cells, *Phys. Rev. E* **47** (1993) 2128.

88. T. Glimm, R. Bhat and S. A. Newman, Modeling the morphodynamic galectin patterning network of the developing avian limb skeleton, *J. Theor. Biol.* **346** (2014) 86–108.

89. B. D. Goddard, B. Gooding, H. Short and G. Pavliotis, Noisy bounded confidence models for opinion dynamics: The effect of boundary conditions on phase transitions, *IMA J. Appl. Math.* **87** (2022) 80–110.

90. M. Golubitsky and I. Stewart, *The Symmetry Perspective*, Progress in Mathematics (Birkhäuser, 2002).

91. X. Gong, M. Herty, B. Piccoli and G. Visconti, Crowd dynamics: Modeling and control of multiagent systems, *Annu. Rev. Control Robot. Auton. Syst.* **6** (2023) 261–282.

92. F. Graner and J. A. Glazier, Simulation of biological cell sorting using a two-dimensional extended Potts model, *Phys. Rev. Lett.* **69** (1992) 2013.

93. J. Green, S. Waters, J. Whiteley, L. Edelstein-Keshet, K. Shakesheff and H. Byrne, Non-local models for the formation of hepatocyte–stellate cell aggregates, *J. Theor. Biol.* **267** (2010) 106–120.

94. D. Grünbaum and A. Okubo, Modelling social animal aggregations, in *Frontiers in Mathematical Biology* (Springer, 1994), pp. 296–325.

95. R. Hegselmann and U. Krause, Opinion dynamics and bounded confidence: Models, analysis and simulation, *J. Artif. Soc. Social Simul.* **5** (2022) 1–33.

96. F. Heppner, A stochastic nonlinear model for coordinated bird flocks, in *The Ubiquity of Chaos* (AAAS Publications, 1990).

97. T. Hillen and A. Buttenschön, Nonlocal adhesion models for microorganisms on bounded domains, *SIAM J. Appl. Math.* **80** (2020) 382–401.

98. T. Hillen and A. Buttenschön, *Non-local Cell Adhesion Models*: *Symmetries and Bifurcations in 1-D* (Springer, 2021).

99. T. Hillen, N. Loy, K.J. Painter, R. Thiessen, *J. Math. Biol*, in press, 2023.

100. T. Hillen and K. J. Painter, A user's guide to PDE models for chemotaxis, *J. Math. Biol.* **58** (2009) 183.

101. T. Hillen and K. J. Painter, Transport and anisotropic diffusion models for movement in oriented habitats, in *Dispersal, Individual Movement and Spatial Ecology*: *A Mathematical Perspective* (Springer, 2013), pp. 177–222.

102. T. Hillen, K. J. Painter and M. Winkler, Global solvability and explicit bounds for non-local adhesion models, *Eur. J. Appl. Math.* **29** (2018) 645–684.

103. A. Hodgkinson, M. A. Chaplain, P. Domschke and D. Trucu, Computational approaches and analysis for a spatio-structural-temporal invasive carcinoma model, *Bull. Math. Biol.* **80** (2018) 701–737.

104. S. Hoehme and D. Drasdo, A cell-based simulation software for multi-cellular systems, *Bioinformatics* **26** (2010) 2641–2642.

105. T. Höfer, J. A. Sherratt and P. K. Maini, *Dictyostelium discoideum*: Cellular self-organization in an excitable biological medium, *Proc. R. Soc. London. Ser. B*: *Biol. Sci.* **259** (1995) 249–257.

106. D. Horstmann, K. J. Painter and H. G. Othmer, Aggregation under local reinforcement: From lattice to continuum, *Eur. J. Appl. Math.* **15** (2004) 545–576.

107. B. D. Hughes, *Random Walks and Random Environments*: *Random Walks*, Vol. 1 (Oxford Univ. Press, 1995).

108. M. Inaba, H. Yamanaka and S. Kondo, Pigment pattern formation by contact-dependent depolarization, *Science* **335** (2012) 677–677.

109. M. Janiszewska, M. C. Primi and T. Izard, Cell adhesion in cancer: Beyond the migration of single cells, *J. Biol. Chem.* **295** (2020) 2495–2505.

110. T. J. Jewell, A. L. Krause, P. K. Maini and E. A. Gaffney, Patterning of nonlocal transport models in biology: The impact of spatial dimension, *Math. Biosci.* **366** (2023) 109093.

111. S. T. Johnston, M. J. Simpson and R. E. Baker, Mean-field descriptions of collective migration with strong adhesion, *Phys. Rev. E* **85** (2012) 051922.

112. S. T. Johnston, M. J. Simpson and D. S. McElwain, How much information can be obtained from tracking the position of the leading edge in a scratch assay?, *J. R. Soc. Interface* **11** (2014) 20140325.

113. S. T. Johnston, M. J. Simpson, D. S. McElwain, B. J. Binder and J. V. Ross, Interpreting scratch assays using pair density dynamics and approximate Bayesian computation, *Open Biol.* **4** (2014) 140097.

114. S. T. Johnston, M. J. Simpson and M. J. Plank, Lattice-free descriptions of collective motion with crowding and adhesion, *Phys. Rev. E* **88** (2013) 062720.

115. J. W. Jolles, A. J. King and S. S. Killen, The role of individual heterogeneity in collective animal behaviour, *Trends Ecol. Evol.* **35** (2020) 278–291.

116. K. Kawasaki, Diffusion and the formation of spatial distributions, *Math. Sci.* **16** (1978) 47–52.

117. E. F. Keller and L. A. Segel, Initiation of slime mold aggregation viewed as an instability, *J. Theor. Biol.* **26** (1970) 399–415.

118. J. Kennedy and R. Eberhart, Particle swarm optimization, in *Proc. ICNN'95 — Int. Conf. Neural Networks*, Vol. 4 (IEEE, 1995), pp. 1942–1948.

119. Y. Kim, S. Lawler, M. O. Nowicki, E. A. Chiocca and A. Friedman, A mathematical model for pattern formation of glioma cells outside the tumor spheroid core, *J. Theor. Biol.* **260** (2009) 359–371.

120. J. A. King, The ecology of aggressive behavior, *Annu. Rev. Ecol. Syst.* **4** (1973) 117–138.

121. H. Knútsdóttir, E. Pálsson and L. Edelstein-Keshet, Mathematical model of macrophage-facilitated breast cancer cells invasion, *J. Theor. Biol.* **357** (2014) 184–199.

122. O. Korenkova, A. Pepe and C. Zurzolo, Fine intercellular connections in development: TNTs, cytonemes, or intercellular bridges? *Cell Stress* **4** (2020) 30.

123. B. Kvokačková, J. Remšík, M. K. Jolly and K. Souček, Phenotypic heterogeneity of triple-negative breast cancer mediated by epithelial–mesenchymal plasticity, *Cancers* **13** (2021) 2188.

124. T. Laurent, Local and global existence for an aggregation equation, *Commun. Partial Differ. Equ.* **32** (2007) 1941–1964.

125. C. Lee, M. Hoopes, J. Diehl, W. Gilliland, G. Huxel, E. Leaver, K. McCann, J. Umbanhowar and A. Mogilner, Non-local concepts and models in biology, *J. Theor. Biol.* **210** (2001) 201–219.

126. M. A. Lewis, S. V. Petrovskii and J. R. Potts, *The Mathematics behind Biological Invasions*, Vol. 44 (Springer, 2016).

127. M. Lizana and V. Padron, A spatially discrete model for aggregating populations, *J. Math. Biol.* **38** (1999) 79–102.

128. C.-Y. Loh, J. Y. Chai, T. F. Tang, W. F. Wong, G. Sethi, M. K. Shanmugam, P. P. Chong and C. Y. Looi, The e-cadherin and n-cadherin switch in epithelial-to-mesenchymal transition: Signaling, therapeutic implications, and challenges, *Cells* **8** (2019) 1118.

129. F. Lu, M. Zhong, S. Tang and M. Maggioni, Nonparametric inference of interaction laws in systems of agents from trajectory data, *Proc. Natl. Acad. Sci.* **116** (2019) 14424–14433.

130. F. Lutscher, *Integrodifference Equations in Spatial Ecology* (Springer, 2020).

131. P. Macklin, M. E. Edgerton, A. M. Thompson and V. Cristini, Patient-calibrated agent-based modelling of ductal carcinoma in situ (DCIS): From microscopic measurements to macroscopic predictions of clinical progression, *J. Theor. Biol.* **301** (2012) 122–140.

132. N. C. Makris, P. Ratilal, S. Jagannathan, Z. Gong, M. Andrews, I. Bertsatos, O. R. Godø, R. W. Nero and J. M. Jech, Critical population density triggers rapid formation of vast oceanic fish shoals, *Science* **323** (2009) 1734–1737.

133. Y. Matsunaga, M. Noda, H. Murakawa, K. Hayashi, A. Nagasaka, S. Inoue, T. Miyata, T. Miura, K.-i. Kubo and K. Nakajima, Reelin transiently promotes n-cadherin-dependent neuronal adhesion during mouse cortical development, *Proc. Natl. Acad. Sci.* **114** (2017) 2048–2053.

134. P. Matthews and S. M. Cox, Pattern formation with a conservation law, *Nonlinearity* **13** (2000) 1293.

135. R. Mayor and S. Etienne-Manneville, The front and rear of collective cell migration, *Nat. Rev. Mol. Cell Biol.* **17** (2016) 97–109.

136. R. McLennan *et al.*, Neural crest cells bulldoze through the microenvironment using aquaporin 1 to stabilize filopodia, *Development* **147** (2020) dev185231.

137. J. Merkle, D. Fortin and J. M. Morales, A memory-based foraging tactic reveals an adaptive mechanism for restricted space use, *Ecol. Lett.* **17** (2014) 924–931.

138. J. A. Merkle, J. R. Potts and D. Fortin, Energy benefits and emergent space use patterns of an empirically parameterized model of memory-based patch selection, *Oikos* **126** (2017) 185–195.

139. A. M. Middleton, C. Fleck and R. Grima, A continuum approximation to an off-lattice individual-cell based model of cell migration and adhesion, *J. Theor. Biol.* **359** (2014) 220–232.

140. M. Mimura and M. Yamaguti, Pattern formation in interacting and diffusing systems in population biology, *Adv. Biophys.* **15** (1982) 19–65.

141. G. R. Mirams *et al.*, Chaste: An open source C++ library for computational physiology and biology, *PLoS Comput. Biol.* **9** (2013) e1002970.

142. V. Miskolci, L. C. Klemm and A. Huttenlocher, Cell migration guided by cell–cell contacts in innate immunity, *Trends in Cell Biol.* **31** (2021) 86–94.

143. A. Mogilner and L. Edelstein-Keshet, A non-local model for a swarm, *J. Math. Biol.* **38** (1999) 534–570.

144. P. R. Moorcroft, M. A. Lewis and R. L. Crabtree, Mechanistic home range models capture spatial patterns and dynamics of coyote territories in yellowstone, *Proc. R. Soc. B* **273** (2006) 1651–1659.

145. D. Morale, V. Capasso and K. Oelschläger, An interacting particle system modelling aggregation behavior: From individuals to populations, *J. Math. Biol.* **50** (2005) 49–66.

146. S. Motsch and E. Tadmor, A new model for self-organized dynamics and its flocking behavior, *J. Stat. Phys.* **144** (2011) 923–947.

147. S. Motsch and E. Tadmor, Heterophilious dynamics enhances consensus, *SIAM Rev.* **56** (2014) 577–621.

148. R. Munden, L. Börger, R. P. Wilson, J. Redcliffe, R. Brown, M. Garel and J. R. Potts, Why did the animal turn? Time-varying step selection analysis for inference between observed turning-points in high frequency data, *Methods Ecol. Evol.* **12** (2021) 921–932.

149. H. Murakawa and H. Togashi, Continuous models for cell–cell adhesion, *J. Theor. Biol.* **374** (2015) 1–12.

150. J. D. Murray, *Mathematical Biology. II. Spatial Models and Biomedical Applications* (Springer, 2003).

151. T. Nagai and M. Mimura, Asymptotic behavior for a nonlinear degenerate diffusion equation in population dynamics, *SIAM J. Appl. Math.* **43** (1983) 449–464.

152. A. Okubo, S. A. Levin, A. Okubo, D. Grünbaum and L. Edelstein-Keshet, The dynamics of animal grouping, in *Diffusion and Ecological Problems*: *Modern Perspectives* (Springer, 2001), pp. 197–237.

153. J. M. Osborne, A. G. Fletcher, J. M. Pitt-Francis, P. K. Maini and D. J. Gavaghan, Comparing individual-based approaches to modelling the self-organization of multicellular tissues, *PLoS Comput. Biol.* **13** (2017) e1005387.

154. M. Osswald *et al.*, Brain tumour cells interconnect to a functional and resistant network, *Nature* **528** (2015) 93–98.

155. H. G. Othmer, S. R. Dunbar and W. Alt, Models of dispersal in biological systems, *J. Math. Biol.* **26** (1988) 263–298.

156. K. J. Painter, Continuous models for cell migration in tissues and applications to cell sorting via differential chemotaxis, *Bull. Math. Biol.* **71** (2009) 1117–1147.

157. K. J. Painter, N. J. Armstrong and J. A. Sherratt, The impact of adhesion on cellular invasion processes in cancer and development, *J. Theor. Biol.* **264** (2010) 1057–1067.

158. K. J. Painter, J. Bloomfield, J. Sherratt and A. Gerisch, A nonlocal model for contact attraction and repulsion in heterogeneous cell populations, *Bull. Math. Biol.* **77** (2015) 1132–1165.

159. K. J. Painter and T. Hillen, From random walks to fully anisotropic diffusion models for cell and animal movement, in *Cell Movement*: *Modeling and Applications* (Springer, 2018), pp. 103–141.

160. K. J. Painter, D. Horstmann and H. G. Othmer, Localization in lattice and continuum models of reinforced random walks, *Appl. Math. Lett.* **16** (2003) 375–381.

161. E. Palsson, A 3-d model used to explore how cell adhesion and stiffness affect cell sorting and movement in multicellular systems, *J. Theor. Biol.* **254** (2008) 1–13.

162. E. Palsson and H. G. Othmer, A model for individual and collective cell movement in *Dictyostelium discoideum*, *Proc. Natl. Acad. Sci.* **97** (2000) 10448–10453.

163. C. S. Patlak, Random walk with persistence and external bias, *Bull. Math. Biophys.* **15** (1953) 311–338.

164. K. Pearson, The problem of the random walk, *Nature* **72** (1905) 294–294.

165. B. Perthame, *Transport Equations in Biology* (Springer Science & Business Media, 2006).

166. B. Pettit, Z. Akos, T. Vicsek and D. Biro, Speed determines leadership and leadership determines learning during pigeon flocking, *Curr. Biol.* **25** (2015) 3132–3137.

167. J. P. Pinasco, V. Semeshenko and P. Balenzuela, Modeling opinion dynamics: Theoretical analysis and continuous approximation, *Chaos Solitons Fractals* **98** (2017) 210–215.

168. J. Potts, T. Hillen and M. Lewis, The "edge effect" phenomenon: Deriving population abundance patterns from individual animal movement decisions, *Theor. Ecol.* **9** (2016) 233–247.

169. J. R. Potts, G. Bastille-Rousseau, D. L. Murray, J. A. Schaefer and M. A. Lewis, Predicting local and non-local effects of resources on animal space use using a mechanistic step selection model, *Methods Ecol. Evol.* **5** (2014) 253–262.

170. J. R. Potts and L. Börger, How to scale up from animal movement decisions to spatiotemporal patterns: An approach via step selection, *J. Anim. Ecol.* **92** (2023) 16–29.

171. J. R. Potts, L. Börger, B. K. Strickland and G. M. Street, Assessing the predictive power of step selection functions: How social and environmental interactions affect animal space use, *Methods Ecol. Evol.* **13** (2022) 1805–1818.

172. J. R. Potts and M. A. Lewis, How do animal territories form and change? Lessons from 20 years of mechanistic modelling, *Proc. R. Soc. B*: *Biol. Sci.* **281** (2014) 20140231.

173. J. R. Potts and M. A. Lewis, How memory of direct animal interactions can lead to territorial pattern formation, *J. R. Soc. Interface* **13** (2016) 20160059.

174. J. R. Potts and M. A. Lewis, Territorial pattern formation in the absence of an attractive potential, *J. Math. Biol.* **72** (2016) 25–46.

175. J. R. Potts and M. A. Lewis, Spatial memory and taxis-driven pattern formation in model ecosystems, *Bull. Math. Biol.* **81** (2019) 2725–2747.

176. J. R. Potts, K. Mokross and M. A. Lewis, A unifying framework for quantifying the nature of animal interactions, *J. R. Soc. Interface* **11** (2014) 20140333.

177. J. R. Potts and U. E. Schlägel, Parametrizing diffusion-taxis equations from animal movement trajectories using step selection analysis, *Methods Ecol. Evol.* **11** (2020) 1092–1105.

178. P. Rabinowitz, Some global results for nonlinear eigenvalue problems, *J. Funct. Anal.* **513** (1971) 487–513.

179. C. W. Reynolds, "Flocks, herds and schools: A distributed behavioral model", *Comput Graph.* **21** (1987) 25–34.

180. L. Riotte-Lambert, S. Benhamou and S. Chamaillé-Jammes, How memory-based movement leads to nonterritorial spatial segregation, *Am. Nat.* **185** (2015) E103–E116.

181. C. Roehlecke and M. H. Schmidt, Tunneling nanotubes and tumor microtubes in cancer, *Cancers* **12** (2020) 857.

182. A. Roussi, Why gigantic locust swarms are challenging governments and researchers., *Nature* **579** (2020) 330–331.

183. T. Sekimura, M. Zhu, J. Cook, P. K. Maini and J. D. Murray, Pattern formation of scale cells in lepidoptera by differential origin-dependent cell adhesion, *Bull. Math. Biol.* **61** (1999) 807–828.

184. J. A. Sherratt, S. A. Gourley, N. J. Armstrong and K. J. Painter, Boundedness of solutions of a non-local reaction–diffusion model for adhesion in cell aggregation and cancer invasion, *Eur. J. Appl. Math.* **20** (2009) 123–144.

185. M. S. Steinberg, Adhesion-guided multicellular assembly: A commentary upon the postulates, real and imagined, of the differential adhesion hypothesis, with special attention to computer simulations of cell sorting, *J. Theor. Biol.* **55** (1975) 431–443.

186. M. S. Steinberg, Differential adhesion in morphogenesis: A modern view, *Curr. Opin. Genet. Dev.* **17** (2007) 281–286.

187. M. S. Steinberg and S. F. Gilbert, Townes and Holtfreter (1955): Directed movements and selective adhesion of embryonic amphibian cells, *J. Exp. Zool. Part A*: *Comp. Exp. Biol.* **301** (2004) 701–706.

188. A. Stevens and H. G. Othmer, Aggregation, blowup, and collapse: The ABC's of taxis in reinforced random walks, *SIAM J. Appl. Math.* **57** (1997) 1044–1081.

189. D. Sulsky, S. Childress and J. Percus, A model of cell sorting, *J. Theor. Biol.* **106** (1984) 275–301.

190. D. J. Sumpter, *Collective Animal Behavior* (Princeton Univ. Press, 2010).

191. S. Suveges, K. Hossain-Ibrahim, J. D. Steele, R. Eftimie and D. Trucu, Mathematical modelling of glioblastomas invasion within the brain: A 3d multi-scale moving-boundary approach, *Mathematics* **9** (2021) 2214.

192. M. H. Swat, G. L. Thomas, J. M. Belmonte, A. Shirinifard, D. Hmeljak and J. A. Glazier, Multi-scale modeling of tissues using CompuCell3D, *Methods Cell Biol.* **110** (2012) 325–366.

193. M. Takeichi, Cell sorting *in vitro* and *in vivo*: How are cadherins involved?, *Semin. Cell Dev. Biol.* **147** (2022) 2–11.

194. N. Tania, B. Vanderlei, J. P. Heath and L. Edelstein-Keshet, Role of social interactions in dynamic patterns of resource patches and forager aggregation, *Proc. Natl. Acad. Sci.* **109** (2012) 11228–11233.

195. G. Theraulaz and E. Bonabeau, A brief history of stigmergy, *Artif. Life* **5** (1999) 97–116.

196. E. Theveneau, B. Steventon, E. Scarpa, S. Garcia, X. Trepat, A. Streit and R. Mayor, Chase-and-run between adjacent cell populations promotes directional collective migration, *Nat. Cell Biol.* **15** (2013) 763–772.

197. H. Thurfjell, S. Ciuti and M. S. Boyce, Applications of step-selection functions in ecology and conservation, *Mov. Ecol.* **2** (2014) 1–12.

198. C. M. Topaz, A. L. Bertozzi and M. A. Lewis, A nonlocal continuum model for biological aggregation, *Bull. Math. Biol.* **68** (2006) 1601–1623.

199. C. M. Topaz, M. R. D'Orsogna, L. Edelstein-Keshet and A. J. Bernoff, Locust dynamics: Behavioral phase change and swarming, *PLoS Comput. Biol.* **8** (2012) e1002642.

200. P. L. Townes and J. Holtfreter, Directed movements and selective adhesion of embryonic amphibian cells, *J. Exp. Zool.* **128** (1955) 53–120.

201. O. Trush *et al.*, N-cadherin orchestrates self-organization of neurons within a columnar unit in the drosophila medulla, *J. Neurosci.* **39** (2019) 5861–5880.

202. T. Y.-C. Tsai, R. M. Garner and S. G. Megason, Adhesion-based self-organization in tissue patterning, *Annu. Rev. Cell Dev. Biol.* **38** (2022) 349–374.

203. P. Turchin, *Quantitative Analysis of Movement*: *Measuring and Modeling Population Redistribution in Animals and Plants* (Sinauer, 1998).
204. A. M. Turing, The chemical basis of morphogenesis, *Philos. Trans. R. Soc. London B* **237** (1952) 37–72.
205. N. G. Van Kampen, *Stochastic Processes in Physics and Chemistry*, Vol. 1 (Elsevier, 1992).
206. P. Van Liedekerke, M. Palm, N. Jagiella and D. Drasdo, Simulating tissue mechanics with agent-based models: Concepts, perspectives and some novel results, *Comput. Part. Mech.* **2** (2015) 401–444.
207. B. Van Moorter, D. Visscher, S. Benhamou, L. Börger, M. S. Boyce and J.-M. Gaillard, Memory keeps you at home: A mechanistic model for home range emergence, *Oikos* **118** (2009) 641–652.
208. T. Vicsek, A. Czirók, E. Ben-Jacob, I. Cohen and O. Shochet, Novel type of phase transition in a system of self-driven particles, *Phys. Rev. Lett.* **75** (1995) 1226.
209. T. Vicsek and A. Zafeiris, Collective motion, *Phys. Rep.* **517** (2012) 71–140.
210. C. Villa, A. Gerisch and M. A. Chaplain, A novel nonlocal partial differential equation model of endothelial progenitor cell cluster formation during the early stages of vasculogenesis, *J. Theor. Biol.* **534** (2022) 110963.
211. H. Wang and Y. Salmaniw, "Open problems in PDE models for knowledge-based animal movement via nonlocal perception and cognitive mapping", *J. Math. Biol.* **86** (2023) 71.
212. A. J. Ward, P. Thomas, P. J. Hart and J. Krause, Correlates of boldness in three-spined sticklebacks (*Gasterosteus aculeatus*), *Behav. Ecol. Sociobiol.* **55** (2004) 561–568.
213. G. Webb, The force of cell–cell adhesion in determining the outcome in a nonlocal advection diffusion model of wound healing, *Math. Biosci. Eng.* **19** (2022) 8689–8704.
214. G. Webb and X. E. Zhao, Bifurcation analysis of critical values for wound closure outcomes in wound healing experiments, *J. Math. Biol.* **86** (2023) 1–26.
215. H. J. Williams *et al.*, Optimizing the use of biologgers for movement ecology research, *J. Anim. Ecol.* **89** (2020) 186–206.
216. R. Wilson, I. Griffiths, P. Legg, M. Friswell, O. Bidder, L. Halsey, S. A. Lambertucci and E. Shepard, Turn costs change the value of animal search paths, *Ecol. Lett.* **16** (2013) 1145–1150.
217. S. M. Wise, J. S. Lowengrub, H. B. Frieboes and V. Cristini, Three-dimensional multispecies nonlinear tumor growth — I: Model and numerical method, *J. Theor. Biol.* **253** (2008) 524–543.
218. K. Wolf, M. M. Zegers and P. Friedl, Collective cell migration: Guidance principles and hierarchies, *Trends Cell Biol.* **25** (2015) 556–566.
219. H. Yamanaka and S. Kondo, *In vitro* analysis suggests that difference in cell movement during direct interaction can generate various pigment patterns *in vivo*, *Proc. Natl. Acad. Sci.* **111** (2014) 1867–1872.
220. Y. M. Yamashita, M. Inaba and M. Buszczak, Specialized intercellular communications via cytonemes and nanotubes, *Annu. Rev. Cell Dev. Biol.* **34** (2018) 59–84.